



# MIT Open Access Articles

## *Port reduction in parametrized component static condensation: approximation and a posteriori error estimation*

The MIT Faculty has made this article openly available. **Please share** how this access benefits you. Your story matters.

<b>Citation</b>	Eftang, Jens L., and Anthony T. Patera. "Port Reduction in Parametrized Component Static Condensation: Approximation and a Posteriori Error Estimation." <i>Int. J. Numer. Meth. Engng</i> (July 2013): n/a-n/a.
<b>As Published</b>	<a href="http://dx.doi.org/10.1002/nme.4543">http://dx.doi.org/10.1002/nme.4543</a>
<b>Publisher</b>	Wiley Blackwell
<b>Version</b>	Original manuscript
<b>Citable link</b>	<a href="http://hdl.handle.net/1721.1/97696">http://hdl.handle.net/1721.1/97696</a>
<b>Terms of Use</b>	Creative Commons Attribution-Noncommercial-Share Alike
<b>Detailed Terms</b>	<a href="http://creativecommons.org/licenses/by-nc-sa/4.0/">http://creativecommons.org/licenses/by-nc-sa/4.0/</a>

# Port Reduction in Parametrized Component Static Condensation: Approximation and *A Posteriori* Error Estimation\*

Jens L. Eftang<sup>†</sup>

Anthony T. Patera<sup>†</sup>

## Abstract

We introduce a port (interface) approximation and a *a posteriori* error bound framework for a general component-based static condensation method in the context of parameter-dependent linear elliptic partial differential equations. The key ingredients are *i*) efficient *empirical* port approximation spaces — the dimensions of these spaces may be chosen small in order to reduce the computational cost associated with formation and solution of the static condensation system, and *ii*) a computationally tractable *a posteriori* error bound realized through a non-conforming approximation and associated conditioner — the error in the global system approximation, or in a scalar output quantity, may be bounded relatively sharply with respect to the underlying finite element discretization.

Our approximation and *a posteriori* error bound framework is of particular computational relevance for the static condensation reduced basis element (SCRBE) method. We provide several numerical examples within the SCRBE context which serve to demonstrate the convergence rate of our port approximation procedure as well as the efficacy of our port reduction error bounds.

**Keywords:** static condensation; reduced basis element method; component synthesis; domain decomposition; port reduction; interface reduction; *a posteriori* error estimation; non-conforming methods

## 1 Introduction

In many design and engineering applications the physical system under consideration admits a natural component-based synthesis. Examples are particularly ubiquitous in the area of structural analysis: buildings, bridges, space satellites, and other frame-based structures are typically comprised of many and often identical or at least very similar components. Examples of component-based systems may also be found in other areas such as heat transfer and acoustics: heat exchanger systems [28] typically consist of a large number of interconnected pipes and bifurcations; sound mitigation systems may be beneficially considered as a collection of waveguide elements [14, 16].

A popular approach to component-based analysis is the classical component mode synthesis (CMS) method [9, 13]. In this approach, a standard static condensation procedure is performed to eliminate an eigenmodal expansion of the component-interior “bubble” degrees of freedom in terms of many fewer interface, or “port,” degrees of freedom associated with a Schur complement system. Although the original CMS methods [9, 13] do not consider reduction of the degrees of freedom associated with the ports, more recent work considers several port economizations (or interface reduction strategies): an eigenmode expansion (with subsequent truncation) for the port degrees of freedom is proposed in [6, 12]; an adaptive port reduction procedure based on *a posteriori* error estimators for the port reduction is proposed in [18]; and an alternative port reduction approach, with a different bubble function approximation space, is proposed for time-dependent problems in [3].

---

\*Revised preprint submitted May 30, 2013, to International Journal for Numerical Methods in Engineering (Wiley).

<sup>†</sup>Department of Mechanical Engineering, Massachusetts Institute of Technology. 77 Massachusetts Avenue, Cambridge, MA-02139, USA. {eftang, patera}@mit.edu

In the context of *parameter-dependent* partial differential equations, the reduced basis element (RBE) method [20, 21] provides a component-based approximation framework. In the RBE approach, a reduced basis (RB) approximation [25] in the component interiors provides a rapidly convergent local (“bubble”) approximation for any value of the component parameters. However, the components are coupled not by static condensation but rather through a mortar-type procedure at the ports; port truncation may thus be readily introduced through the mortar (continuity Lagrange multiplier) spaces.

The static condensation reduced basis element (SCRBE) method recently introduced in [15] combines concepts from both RBE and CMS: the component bubble functions are approximated by an RB expansion while the component coupling is effected through a static condensation procedure. A key advantage of the SCRBE procedure — an advantage we wish to preserve here — is the interoperability of components and hence the ability to synthesize many (very) different systems from a single library of parametrized components. We note that the SCRBE (as well as CMS, and more generally approaches based on static condensation) is limited to linear problems such as the elliptic partial differential equations which describe linear elasticity, heat transfer, or frequency-domain acoustics.

For large component-based problems, in particular with three-dimensional domains and vector-valued fields, the number of degrees of freedom associated with the ports (that is, the size of the Schur complement system) limits the computational efficacy of the SCRBE. We can not directly apply CMS port reduction concepts in the parameter-dependent context [10], as the chosen port modes must be able to provide a good representation of the solution for any value of the parameters. In this paper, we introduce a port approximation and *a posteriori* error bound framework for a general component-based static condensation method in the context of parameter-dependent linear elliptic partial differential equations.

For this general method we present two key innovations. The first innovation is an algorithm for construction of efficient (small) port approximation spaces which provide good solution accuracy with relatively few modes, and hence reduce the computational complexity associated with formation and solution of the static condensation system — particularly important for large three-dimensional systems with vector-valued fields. The second innovation is a computationally tractable *a posteriori* bound for the error in the solution to the Schur complement system due to port reduction — the error is bounded with respect to an underlying finite element (FE) discretization in the standard functional energy norm, or for associated outputs of interest.

The port reduction framework presented here improves our earlier work [10] in two critical ways. First, to accommodate topological flexibility, our port modes here shall be tailored not to a particular system of components but rather to a particular component and its possible connections to other components. Second, for sharp *a posteriori* error estimation, our error bound here is based on a computationally tractable non-conforming approximation to the exact error rather than direct residual evaluation; the former provides an approximate solution to the error-residual equation and thus avoids the Cauchy-Schwarz inequality of the latter — we thus expect a significantly sharper bound here compared to our earlier approach [10].

We emphasize that in our port reduction procedure we realize computational savings through reduction of the number of interface degrees of freedom and hence the size of the Schur complement system *in combination* with a bubble function approximation (here provided by the SCRBE) which effectively eliminates the interior degrees of freedom. This approach is thus very different from other (iterative or parallel) domain decomposition solution methods [27], in which many local FE solves replace one very large global FE solve. In this latter context the goal is to obtain the exact solution of the original FE-discretized problem through an efficient solution algorithm; however the number of degrees of freedom is not fundamentally reduced.

The remainder of this paper is organized as follows. In the next section we describe a general component-based static condensation framework; we also briefly recall the SCRBE method [15], which provides the bubble function approximations for our numerical examples. In Section 3 we introduce our port approximation and reduction framework, and in Section 4 we develop the *a posteriori* error bound for our port-reduced static condensation approximation. In Section 5 we discuss the relevant computational procedures and costs. In Section 6 we illustrate our procedure through a numerical example, and finally, in Section 7 we provide some concluding remarks.

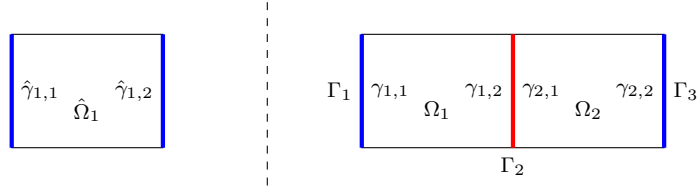


Figure 1: A library with  $M = 1$  archetype component (left): the archetype domain is  $\hat{\Omega}_1$  and has two local ports  $\hat{\gamma}_{1,1}, \hat{\gamma}_{1,2}$ . A system consisting of  $I = 2$  instantiations of the archetype (right): the component domains  $\Omega_1$  and  $\Omega_2$  are instantiations of  $\hat{\Omega}_1$ . The two components are connected at the shared global port  $\Gamma_2$ ; the system has boundary global ports  $\Gamma_1$  and  $\Gamma_3$ ; the local ports are indicated in the domain interiors. Here,  $\mathcal{M}(i) = 1$  for  $i = 1, 2$  and  $\pi_1 = \{(1, 1)\}, \pi_2 = \{(1, 2), (2, 1)\}, \pi_3 = \{(2, 2)\}$ .

## 2 Component-Based Static Condensation

In this section we formulate a general static condensation framework for FE discretizations of component-based systems. Our point of view shall be “bottom-up:” we start with (FE-discretized) component domains, which we interconnect at (conforming) predefined ports in order to form a global system domain; we then apply static condensation to the global system to eliminate the component-local (bubble) degrees of freedom in terms of the port degrees of freedom; finally, we solve the smaller Schur complement system.

The formation of the Schur complement requires a large number of component-local FE bubble solves. To reduce the associated computational complexity a model order reduction technique may be applied; for our numerical results in this paper we pursue the SCRBE method [15], which replaces the local FE bubble spaces with much smaller RB [25] spaces. The notation and nomenclature in this section is borrowed from [15] with some simplifications related to the absence here (for simplicity) of parametrized geometries. We recall the main concepts of the SCRBE as regards RB bubble approximation in Section 2.3.

### 2.1 System from Components and Ports

We introduce a *component library* consisting of  $M$  *archetype* components. Each archetype component has an associated physical domain  $\hat{\Omega}_m$  and a set of parameters  $\hat{\mu}_m \in \hat{\mathcal{D}}_m \subset \mathbb{R}^{\hat{P}_m}$ ,  $1 \leq m \leq M$ . Each archetype component domain boundary  $\partial\hat{\Omega}_m$  has a set of  $n_m^\gamma$  disjoint archetype component *local ports*, denoted as  $\hat{\gamma}_{m,j} \subseteq \partial\hat{\Omega}_m$ ,  $1 \leq j \leq n_m^\gamma$ ; we shall assume for simplicity that all ports on a component are separated by non-port, non-Dirichlet boundary segments as the alternative would necessitate additional ingredients (we comment whenever significant modifications to our procedures are required). To each archetype component we shall also associate parameter-dependent bilinear and linear forms  $\hat{a}_m(\cdot, \cdot; \hat{\mu}_m) : H^1(\hat{\Omega}_m) \times H^1(\hat{\Omega}_m) \rightarrow \mathbb{R}$  and  $\hat{f}_m(\cdot; \hat{\mu}_m) : H^1(\hat{\Omega}_m) \rightarrow \mathbb{R}$  which represent the weak form of a parametrized linear elliptic partial differential equation; a discrete space  $X_m^h \subset H^1(\hat{\Omega}_m)$  which corresponds to a standard FE discretization<sup>1</sup> over  $\hat{\Omega}_m$ ; and port spaces  $P_{m,j}^h$  of dimension  $\mathcal{N}_{m,j}^\gamma$  defined as the restriction of  $X_m^h$  to  $\hat{\gamma}_{m,j}$ ,  $1 \leq j \leq n_m^\gamma$ . (See [24] for a summary of the standard function spaces associated with second-order elliptic partial differential equations.)

We next consider a *system* consisting of  $I$  *instantiated* archetype components from the library. We introduce a mapping  $\mathcal{M} : \{1, \dots, I\} \rightarrow \{1, \dots, M\}$  that maps each of the  $I$  component instantiations to one of the  $M$  component archetypes in the library. An instantiated component may connect to at most  $n_{\mathcal{M}(i)}^\gamma$  other instantiated components in the system through its local ports. For  $1 \leq i \leq I$  we introduce the instantiated component domains  $\Omega_i = \mathcal{T}_i(\hat{\Omega}_{\mathcal{M}(i)})$  and the instantiated component local ports  $\gamma_{i,j} = \mathcal{T}_i(\hat{\gamma}_{\mathcal{M}(i),j})$ . Here,  $\mathcal{T}_i : \hat{\Omega}_{\mathcal{M}(i)} \rightarrow \Omega_i$  is a rigid body transformation which ensures that the instantiated components “dock” as desired to their respective component neighbors in the system (more general geometric mappings are considered in [16, 15] but omitted in this paper for simplicity). We shall assume for simplicity that the

<sup>1</sup>Here,  $h > 0$  represents an FE discretization parameter.

archetype bilinear and linear forms do not depend on spatial orientation and hence need not reflect the  $\mathcal{T}_i$  as an argument. Finally, we introduce the instantiated component parameter vectors  $\mu_i = \hat{\mu}_{\mathcal{M}(i)} \in \hat{\mathcal{D}}_{\mathcal{M}(i)}$ .

We may now introduce the physical system domain  $\Omega$  as  $\bar{\Omega} = \cup_{i=1}^I \bar{\Omega}_i$ ; the system parameter domain  $\mathcal{D} \subseteq \oplus_{i=1}^I \hat{\mathcal{D}}_{\mathcal{M}(i)}$ ; and the system parameter  $\mu = (\mu_1, \dots, \mu_I) \in \mathcal{D}$ . Further, we introduce the *global ports*  $\Gamma_p$ ,  $1 \leq p \leq n_0^\Gamma$ , each of which is either the coincidence of two local ports in the interior of  $\Omega$ , or a single local port on the boundary  $\partial\Omega$ . The connectivity of the system shall be defined through index sets  $\pi_p$ ,  $1 \leq p \leq n_0^\Gamma$ . In the case of an interior global port (coincidence of two local ports  $\gamma_{i,j}$  and  $\gamma_{i',j'}$ ), we set  $\pi_p = \{(i,j), (i',j')\}$ ; and in the case of a boundary global port (a single local port  $\gamma_{i,j}$ ), we set  $\pi_p = \{(i,j)\}$ . We also introduce for each instantiated component  $i$ ,  $1 \leq i \leq I$ , a local port to global port mapping  $\mathcal{G}_i$  such that for each local port index  $j$ ,  $1 \leq j \leq n_{\mathcal{M}(i)}^\gamma$ , we have  $\mathcal{G}_i(j) = p$  for  $p$  such that  $(i,j)$  is in  $\pi_p$ . A simple illustration of this component-to-system concept is provided in Figure 1.

We shall require conforming port spaces in the sense that for any global port index  $\pi_p = \{(i,j), (i',j')\}$ , we must have

$$P_{\mathcal{M}(i),j}^h = P_{\mathcal{M}(i'),j'}^h. \quad (1)$$

We denote by  $\mathcal{N}_p^\Gamma = \mathcal{N}_{i,j}^\gamma (= \mathcal{N}_{i',j'}^\gamma)$  the dimension of the port space(s) associated with global port  $p$ ; we then introduce the total number of port unknowns as

$$n_{\text{SC},0} = \sum_{p=1}^{n_0^\Gamma} \mathcal{N}_p^\Gamma. \quad (2)$$

In actual practice we may also impose Dirichlet conditions on global ports. We denote by  $n^\Gamma \leq n_0^\Gamma$  the number of global ports on which Dirichlet conditions are *not* imposed. Hence the total number of port degrees of freedom is

$$n_{\text{SC}} = \sum_{p=1}^{n^\Gamma} \mathcal{N}_p^\Gamma, \quad (3)$$

(hence we consider without loss of generality Dirichlet conditions on global ports  $n^\Gamma + 1, \dots, n_0^\Gamma$ ).

We now introduce our system bilinear form and linear functional: for any  $w, v \in H^1(\Omega)$ ,

$$a(w, v; \mu) = \sum_{i=1}^I a_{\mathcal{M}(i)}(w|_{\Omega_i}, v|_{\Omega_i}; \mu_i), \quad (4)$$

and

$$f(v; \mu) = \sum_{i=1}^I f_{\mathcal{M}(i)}(v|_{\Omega_i}; \mu_i). \quad (5)$$

We shall suppose that, for any  $\mu \in \mathcal{D}$ ,  $a(\cdot, \cdot; \mu)$  is coercive and continuous with respect to the standard  $H^1(\Omega)$  inner product. We may then, for any  $\mu \in \mathcal{D}$ , introduce the solution to the (well-posed) *continuous* system-level problem: find  $u(\mu) \in X(\Omega) \subset H^1(\Omega)$  such that

$$a(u(\mu), v; \mu) = f(v; \mu), \quad \forall v \in X(\Omega), \quad (6)$$

where  $X(\Omega)$  is equal to  $H^1(\Omega)$  except for restrictions related to (port and non-port) Dirichlet boundary conditions. We also introduce an output of interest associated with our system as  $s(\mu) = \ell(u(\mu); \mu)$  for an  $X(\Omega)$ -bounded linear output functional  $\ell(\cdot; \mu)$ .

Finally, we introduce our discrete FE system-level problem (to which we shall apply static condensation). The discrete system FE space  $X^h(\Omega) \subset X(\Omega)$  is given as  $X^h(\Omega) = (\oplus_{i=1}^I X_{\mathcal{M}(i)}^h) \cap X(\Omega)$ ; hence  $X^h(\Omega)$

inherits the boundary conditions and global continuity enforced by  $X(\Omega)$ . We then define, for any  $\mu \in \mathcal{D}$ , the FE approximation  $u^h(\mu)$  to  $u(\mu)$ :  $u^h(\mu) \in X^h(\Omega)$  satisfies

$$a(u^h(\mu), v; \mu) = f(v; \mu), \quad \forall v \in X^h(\Omega); \quad (7)$$

and the associated FE output of interest is  $s^h(\mu) = \ell(u^h(\mu); \mu)$ . We assume that  $X^h(\Omega)$  is sufficiently rich that in subsequent error analysis we can neglect the error in  $u^h(\mu)$  and  $s^h(\mu)$  relative to  $u(\mu)$  and  $s(\mu)$ , respectively.

## 2.2 Static Condensation

To formulate our static condensation procedure we first introduce the ‘‘bubble’’ spaces associated with each archetype component domain as

$$B_{m;0}^h \equiv \{v \in X_m^h : v|_{\hat{\gamma}_{m,j}} = 0, \quad 1 \leq j \leq n_m^\gamma\}, \quad 1 \leq m \leq M. \quad (8)$$

We also introduce the basis functions for the port space  $P_{m,j}^h$  as  $\{\chi_{m,j,1}, \dots, \chi_{m,j,\mathcal{N}_{m,j}^\gamma}\}$ ,  $1 \leq j \leq n_m^\gamma$ ,  $1 \leq m \leq M$ . We must require that for any global port index  $\pi_p = \{(i, j), (i', j')\}$ , we have

$$\chi_{\mathcal{M}(i),j,k} = \chi_{\mathcal{M}(i'),j',k}, \quad 1 \leq k \leq \mathcal{N}_p^\Gamma. \quad (9)$$

The particular choice for these functions is critical in the context of port reduction and will be described in more detail in Section 3.

For instantiated component  $i$  in our system,  $1 \leq i \leq I$ , and given the component parameter  $\mu_i$ , we now introduce the functions

$$\phi_{i,j,k}^h(\mu) \equiv b_{i,j,k}^h(\mu) + \psi_{\mathcal{M}(i),j,k}, \quad (10)$$

where the ‘‘bubble functions’’  $b_{i,j,k}^h(\mu_i) \in B_{\mathcal{M}(i);0}^h$ ,  $1 \leq k \leq \mathcal{N}_{\mathcal{M}(i),j}^\gamma$ ,  $1 \leq j \leq n_{\mathcal{M}(i)}^\gamma$ , satisfy

$$a_{\mathcal{M}(i)}(b_{i,j,k}^h(\mu_i), v; \mu_i) = -a_{\mathcal{M}(i)}(\psi_{\mathcal{M}(i),j,k} \circ \mathcal{T}_i^{-1}, v; \mu_i), \quad \forall v \in B_{\mathcal{M}(i);0}^h, \quad (11)$$

and the  $\psi_{m,j,k}$  are extensions<sup>2</sup> of the  $\chi_{m,j,k}$  into the interior of  $\hat{\Omega}_m$  which are zero on  $\hat{\gamma}_{m,j'}$  for  $j' \neq j$  (note since we consider in this paper only simple geometric mappings we shall henceforth take the concatenation with the simple map from instantiated to archetype coordinates,  $[\cdot] \circ \mathcal{T}_i^{-1}$ , as understood). We also introduce a bubble function associated with the component right-hand side,  $b_i^{f;h}(\mu_i) \in B_{\mathcal{M}(i);0}^h$ , which satisfies

$$a_{\mathcal{M}(i)}(b_i^{f;h}(\mu_i), v; \mu_i) = f_{\mathcal{M}(i)}(v; \mu_i), \quad \forall v \in B_{\mathcal{M}(i);0}^h. \quad (12)$$

On each instantiated component, we may then express the solution to (7) as

$$u^h(\mu)|_{\Omega_i} = b_i^{f;h}(\mu_i) + \sum_{j=1}^{n_{\mathcal{M}(i)}^\gamma} \sum_{k=1}^{\mathcal{N}_{\mathcal{M}(i),j}^\gamma} \mathbb{U}_{\mathcal{G}_i(j),k}(\mu) \phi_{i,j,k}^h(\mu_i), \quad (13)$$

for coefficients  $\mathbb{U}_{p,k}(\mu)$ ,  $1 \leq k \leq \mathcal{N}_p^\Gamma$ ,  $1 \leq p \leq n^\Gamma$ , to be determined below.

We shall also require ‘‘patched’’ versions of  $\phi_{i,j,k}$  over pairs of instantiated components connected at global ports: for an interior global port  $\pi_p = \{(i, j), (i', j')\}$  we define  $\Phi_{p,k} \equiv \phi_{i',j',k} + \phi_{i,j,k}$ , while for a boundary global port  $\pi_p = \{(i, j)\}$  we define  $\Phi_{p,k} \equiv \phi_{i,j,k}$ ; note to avoid the heavier (direct sum) notation of [15] we assume here and below that all functions are extended by zero outside their domain of definition.

<sup>2</sup>We employ the usual (discrete) harmonic extensions since in the context of RB approximation this provides for a more economical RB approximation [11].

We may now express the *global* solution as

$$u^h(\mu) = \sum_{i=1}^I b_i^{f;h}(\mu_i) + \sum_{p=1}^{n^\Gamma} \sum_{k=1}^{\mathcal{N}_p^\Gamma} \mathbb{U}_{p,k}(\mu) \Phi_{p,k}(\mu). \quad (14)$$

We then insert (14) into (7) and restrict the test functions to the “skeleton” space

$$\mathcal{S} \equiv \text{span}\{\Phi_{p,k}(\mu), \quad 1 \leq k \leq \mathcal{N}_p^\Gamma, 1 \leq p \leq n^\Gamma\} \subset X^h \quad (15)$$

to obtain the Schur complement system of size  $n_{\text{SC}}$ : for any  $\mu \in \mathcal{D}$ , find  $\mathbb{U}(\mu) \in \mathbb{R}^{n_{\text{SC}}}$  such that

$$\mathbb{A}(\mu)\mathbb{U}(\mu) = \mathbb{F}(\mu), \quad (16)$$

where

$$\mathbb{A}_{(p,k),(p',k')}(\mu) = a(\Phi_{p',k'}(\mu), \Phi_{p,k}(\mu); \mu), \quad (17)$$

$$\mathbb{F}_{(p,k)}(\mu) = f(\Phi_{p,k}(\mu); \mu) - \sum_{i=1}^I a(b_i^{f;h}(\mu_i), \Phi_{p,k}(\mu); \mu), \quad (18)$$

for  $1 \leq k \leq \mathcal{N}_p^\Gamma$ ,  $1 \leq k' \leq \mathcal{N}_{p'}^\Gamma$ ,  $1 \leq p, p' \leq n^\Gamma$  (hence  $(p, k)$  is a double-index notation for a single degree of freedom). Note that any port (and non-port) Dirichlet boundary conditions are already reflected in (14) and (15) and hence also in (16).

---

**Algorithm 1** Component-based static condensation assembly loop

---

$\mathbb{F}_0(\mu) = \mathbf{0}$ ,  $\mathbb{A}_0(\mu) = \mathbf{0}$

**for**  $i = 1, \dots, I$  **do**

**for**  $j = 1, \dots, n_{\mathcal{M}(i)}^\gamma$  **do**

**for**  $k = 1, \dots, \mathcal{N}_{\mathcal{M}(i),j}^\gamma$  **do**

$\mathbb{F}_{0;\mathcal{G}_i(j),k}(\mu) \leftarrow \mathbb{F}_{0;\mathcal{G}_i(j),k}(\mu) + \mathbb{F}_{j,k}^i(\mu_i)$

**for**  $j' = 1, \dots, n_{\mathcal{M}(i)}^\gamma$  **do**

**for**  $k' = 1, \dots, \mathcal{N}_{\mathcal{M}(i),j'}^\gamma$  **do**

$\mathbb{A}_{0;(\mathcal{G}_i(j),k),(\mathcal{G}_i(j'),k')}(\mu) \leftarrow \mathbb{A}_{0;(\mathcal{G}_i(j),k),(\mathcal{G}_i(j'),k')}(\mu) + \mathbb{A}_{(j,k),(j',k')}^i(\mu_i)$

**end for**

**end for**

**end for**

**end for**

**end for**

Eliminate port Dirichlet degrees of freedom:  $\mathbb{F}_0(\mu) \rightarrow \mathbb{F}(\mu)$  and  $\mathbb{A}_0(\mu) \rightarrow \mathbb{A}(\mu)$

---

For the assembly of  $\mathbb{A}(\mu)$  and  $\mathbb{F}(\mu)$  we may employ a direct stiffness procedure. For each component instantiation we define the local “stiffness matrix” and “load vector” as

$$\mathbb{A}_{(j,k),(j',k')}^i(\mu_i) = a_{\mathcal{M}(i)}(\phi_{i,j',k'}(\mu_i), \phi_{i,j,k}(\mu_i); \mu_i), \quad (19)$$

$$\mathbb{F}_{(j,k)}^i(\mu_i) = f_{\mathcal{M}(i)}(\phi_{i,j,k}(\mu_i); \mu_i) - a_{\mathcal{M}(i)}(b_i^{f;h}(\mu_i), \phi_{i,j,k}(\mu_i); \mu_i),$$

respectively, for  $1 \leq k \leq \mathcal{N}_{\mathcal{M}(i),j}^\gamma$ ,  $1 \leq k' \leq \mathcal{N}_{\mathcal{M}(i),j'}^\gamma$ ,  $1 \leq j, j' \leq n_{\mathcal{M}(i)}^\gamma$ ,  $1 \leq i \leq I$ . From these component quantities we may then first obtain  $\mathbb{A}_0(\mu) \in \mathbb{R}^{n_{\text{SC},0} \times n_{\text{SC},0}}$  and  $\mathbb{F}_0(\mu) \in \mathbb{R}^{n_{\text{SC},0}}$  through Algorithm 1; as a final step in the algorithm we impose any port Dirichlet conditions by elimination of the associated rows and columns to obtain  $\mathbb{A}(\mu) \in \mathbb{R}^{n_{\text{SC}} \times n_{\text{SC}}}$  and  $\mathbb{F}(\mu) \in \mathbb{R}^{n_{\text{SC}}}$ .

**Remark 1.** *The Schur complement matrix  $\mathbb{A}(\mu)$  is symmetric and positive definite (SPD) thanks to symmetry and coercivity of  $a(\cdot, \cdot; \mu)$ , the definition of  $\mathbb{A}(\mu)$  in (17), and linear independence of the  $\Phi_{p,k}(\mu)$ ,  $1 \leq k \leq \mathcal{N}_p^\Gamma$ ,  $1 \leq p \leq n^\Gamma$ .*

### 2.3 Static Condensation Reduced Basis Element Method

In the static condensation reduced basis element (SCRBE) method [15], which we consider for our numerical results in Section 6, each of the FE bubble functions  $b_{i,j,k}^h(\mu_i)$  in (11) and  $b_i^{f;h}(\mu_i)$  in (12) is respectively replaced by an RB approximation [25]. Evaluation of these RB approximations is significantly less expensive (subsequent to an RB “offline” preprocessing step) than evaluation of the original FE quantities, and hence the computational cost associated with the formation of the (now approximate) Schur complement system is significantly reduced.

For  $1 \leq k \leq \mathcal{N}_{\mathcal{M}(i),j}^\gamma$ ,  $1 \leq j \leq n_{\mathcal{M}(i)}$ ,  $1 \leq i \leq I$ , we introduce the RB bubble function approximations

$$\tilde{b}_{i,j,k}(\mu_i) \approx b_{i,j,k}^h(\mu_i), \quad \tilde{b}_i^f(\mu_i) \approx b_i^{f;h}(\mu_i), \quad (20)$$

associated with (11) and (12), respectively, and we define  $\tilde{\phi}_{i,j,k}(\mu_i) \equiv \psi_{\mathcal{M}(i),j,k} + \tilde{b}_{i,j,k}(\mu_i)$  and

$$\tilde{\Phi}_{p,k}(\mu) \equiv \sum_{(i,j) \in \pi_p} \tilde{\phi}_{i,j,k}(\mu_i). \quad (21)$$

We may then define  $\tilde{\mathcal{S}} = \text{span}\{\tilde{\Phi}_{p,k}(\mu), 1 \leq k \leq \mathcal{N}_p^\Gamma, 1 \leq p \leq n^\Gamma\} \subset X^h$  (but note  $\tilde{\mathcal{S}} \not\subseteq \mathcal{S}$ ). These RB approximations in turn lead to the approximate Schur complement system

$$\tilde{\mathbb{A}}(\mu)\tilde{\mathbb{U}}(\mu) = \tilde{\mathbb{F}}(\mu), \quad (22)$$

where  $\tilde{\mathbb{A}}(\mu)$  and  $\tilde{\mathbb{F}}(\mu)$  are defined as in (17) except with the  $\Phi_{p,k}$  replaced by  $\tilde{\Phi}_{p,k}$  and the  $b_i^{f;h}(\mu_i)$  replaced by  $\tilde{b}_i^f(\mu_i)$ . We mention that under suitable (*a posteriori* verifiable) conditions on  $\|\mathbb{U}(\mu) - \tilde{\mathbb{U}}(\mu)\|_2$  the SCRBE system matrix  $\tilde{\mathbb{A}}(\mu)$  is SPD [15, Proposition 4.1]; here,  $\|\cdot\|_2$  refers to the usual Euclidean norm.

Associated with the SCRBE is a favorable offline–online separation of the computations. In the offline stage RB approximation spaces tailored to the parameter dependence of each bubble function within each archetype component are constructed; associated datasets (required online) for the RB approximation and RB error bounds are formed and stored. This stage is computationally expensive. In the online stage, the system is first instantiated from archetype components; then, for the specified parameters, the RB bubble approximations are computed for each instantiated component; next, the Schur complement system (22) is assembled and solved; and finally, an *a posteriori* error bound for  $\tilde{\mathbb{U}}(\mu)$  (as well as for associated output quantities) is computed. This stage is fast since the computational cost does not depend on the dimension of the FE spaces associated with the underlying component-local discretizations; we may thus pursue rapid and topologically and parametrically flexible simulation of possibly rather large systems.

The port approximation and reduction procedure which we discuss in the next section, and which is the main focus of this paper, does not rely on any particular approximation procedure for the bubble functions. However, the computational economies realized by our port reduction procedure do rely heavily on efficient bubble function approximation as provided, for example, by the SCRBE; indeed, we shall invoke the SCRBE for our numerical results in Section 6. We do not go into further details about the SCRBE approach here, but instead refer the interested reader to [15].

In the majority of the remainder of the paper we shall suppose, for any  $\mu \in \mathcal{D}$ , that  $\mathbb{A}(\mu) = \tilde{\mathbb{A}}(\mu)$  and  $\mathbb{F}(\mu) = \tilde{\mathbb{F}}(\mu)$ , that is, that the RB errors are zero. This assumption permits significant simplification of the presentation of our port reduction *a posteriori* error bounds (in Section 4). We defer to Appendix A the incorporation of non-zero RB contribution in the error estimates.

## 3 Port Approximation and Reduction

We introduce here our procedure for the reduction of the number of degrees of freedom on the instantiated component ports and hence the size of the Schur complement system (16). A key concept in this section is *empirical port modes*: port space basis functions which are tailored to the “solution manifold” associated with a particular family of ports that may interconnect. We note that this manifold is ostensibly of very large



dimension<sup>3</sup> since it is induced by all possible topological and parametric variations allowed by the archetype components in the library.

However, in an instantiated system the solution on any given interior global port is “only” influenced by the parameter dependence of the two components which share this port *and* the solution on the non-shared ports of these two components. We shall exploit this observation to explore the solution manifold associated with an archetype component port through a *pairwise training* algorithm. We note that the procedure here improves upon our earlier approach from [10]; in [10], the empirical modes are tailored to a particular instantiated system, which thus limits the topological variety of systems in which the modes provide good approximation; in the current paper, the empirical modes are a property of the archetype library components, and hence may serve in *any* system.

### 3.1 Port-Reduced Static Condensation System

We recall that on port  $j$  on instantiated component  $i$  the full port space is given as

$$P_{\mathcal{M}(i),j}^h = \text{span}\{\chi_{\mathcal{M}(i),j,1}, \dots, \chi_{\mathcal{M}(i),j,\mathcal{N}_{\mathcal{M}(i),j}^\gamma}\}. \quad (23)$$

For each port, we shall choose a desired port space dimension  $n_{\mathbb{A},i,j}^\gamma$  such that  $1 \leq n_{\mathbb{A},i,j}^\gamma \leq \mathcal{N}_{\mathcal{M}(i),j}^\gamma$ . We shall then consider the basis functions  $\chi_{\mathcal{M}(i),j,k}$ ,  $1 \leq k \leq n_{\mathbb{A},i,j}^\gamma$ , as the *active* port modes (hence subscript  $\mathbb{A}$ ); we consider the  $n_{\mathbb{I},i,j}^\gamma = \mathcal{N}_{\mathcal{M}(i),j}^\gamma - n_{\mathbb{A},i,j}^\gamma$  remaining basis functions  $\chi_{\mathcal{M}(i),j,k}$ ,  $n_{\mathbb{A},i,j}^\gamma + 1 \leq k \leq \mathcal{N}_{\mathcal{M}(i),j}^\gamma$ , as *inactive* (hence subscript  $\mathbb{I}$ ). Note that  $\text{span}\{\chi_{\mathcal{M}(i),j,1}, \dots, \chi_{\mathcal{M}(i),j,n_{\mathbb{A},i,j}^\gamma}\} \subseteq P_{\mathcal{M}(i),j}^h$ . For numerical stability [7] of our approximation we require that the  $\chi_{m,j,k}$  are mutually  $L^2(\hat{\gamma}_{m,j})$ -orthonormal, and for solution continuity we again must require  $n_{\mathbb{A},i,j}^\gamma = n_{\mathbb{A},i',j'}^\gamma$  for *global* port  $p$  such that  $(i,j) \in \pi_p$  and  $(i',j') \in \pi_p$ .

We denote by  $n_{\mathbb{A},p}^\Gamma$  and  $n_{\mathbb{I},p}^\Gamma$  the number of active and inactive port modes, respectively, associated with global port  $p$ . For our instantiated system we then introduce

$$n_{\mathbb{A}} \equiv \sum_{p=1}^{n^\Gamma} n_{\mathbb{A},p}^\Gamma, \quad n_{\mathbb{I}} \equiv \sum_{p=1}^{n^\Gamma} n_{\mathbb{I},p}^\Gamma, \quad (24)$$

as the number of total active and total inactive port modes, respectively. Note that  $n_{\mathbb{A}} + n_{\mathbb{I}} = n_{\text{SC}}$ . Next, we assume a particular ordering of the degrees of freedom in (16): we first order the degrees of freedom corresponding to the  $n_{\mathbb{A}}$  active system port modes and then the degrees of freedom corresponding to the  $n_{\mathbb{I}}$  inactive system port modes; we may then interpret (16) as

$$\begin{bmatrix} \mathbb{A}_{\mathbb{A}\mathbb{A}}(\mu) & \mathbb{A}_{\mathbb{A}\mathbb{I}}(\mu) \\ \mathbb{A}_{\mathbb{I}\mathbb{A}}(\mu) & \mathbb{A}_{\mathbb{I}\mathbb{I}}(\mu) \end{bmatrix} \mathbb{U}(\mu) = \begin{bmatrix} \mathbb{F}_{\mathbb{A}}(\mu) \\ \mathbb{F}_{\mathbb{I}}(\mu) \end{bmatrix}, \quad (25)$$

where the four blocks in the system matrix correspond to the different couplings between active and inactive modes; note that  $\mathbb{A}_{\mathbb{A}\mathbb{A}}(\mu) \in \mathbb{R}^{n_{\mathbb{A}} \times n_{\mathbb{A}}}$  and that  $\mathbb{A}_{\mathbb{I}\mathbb{I}}(\mu) \in \mathbb{R}^{n_{\mathbb{I}} \times n_{\mathbb{I}}}$ . Our port-reduced approximation shall be given as the solution to the  $n_{\mathbb{A}} \times n_{\mathbb{A}}$  system

$$\mathbb{A}_{\mathbb{A}\mathbb{A}}(\mu) \mathbb{U}_{\mathbb{A}}(\mu) = \mathbb{F}_{\mathbb{A}}(\mu), \quad (26)$$

in which we may discard the (presumably large)  $\mathbb{A}_{\mathbb{I}\mathbb{I}}(\mu)$  block. (Note, however, that the  $\mathbb{A}_{\mathbb{I}\mathbb{A}}(\mu)$ -block is required later for residual evaluation in the context of a *posteriori* error estimation.)

The field variable associated with the solution vector  $\mathbb{U}_{\mathbb{A}}(\mu)$  is

$$u_{\mathbb{A}}(\mu) = \sum_{i=1}^I b_i^{f;h}(\mu_i) + \sum_{p=1}^{n^\Gamma} \sum_{k=1}^{n_{\mathbb{A},p}^\Gamma} \mathbb{U}_{\mathbb{A},p,k}(\mu) \Phi_{p,k}(\mu), \quad (27)$$

<sup>3</sup>Note that in our FE static condensation context, the dimension is limited by  $\mathcal{N}_{m,j}^\gamma$  for port  $\hat{\gamma}_{m,j}$ .

where  $u_A(\mu) \in X^h(\Omega)$  satisfies

$$a(u_A(\mu), v; \mu) = f(v; \mu), \quad \forall v \in \mathcal{S}_A, \quad (28)$$

where

$$\mathcal{S}_A = \text{span}\{\Phi_{p,k}, \quad 1 \leq p \leq n^\Gamma, 1 \leq k \leq n_{A,p}^\Gamma\} \subseteq \mathcal{S} \quad (29)$$

is the port-reduced (or ‘‘active’’) skeleton space.

Finally, we note that when we employ the SCRBE for RB bubble function approximation we must replace  $u_A(\mu)$  by

$$\tilde{u}_A(\mu) = \sum_{i=1}^I \tilde{b}_i^{f;h}(\mu_i) + \sum_{p=1}^{n^\Gamma} \sum_{k=1}^{n_{A,p}^\Gamma} \tilde{U}_{A,p,k}(\mu) \tilde{\Phi}_{p,k}(\mu), \quad (30)$$

where  $\tilde{u}_A(\mu) \in X^h(\Omega)$  satisfies

$$a(\tilde{u}_A(\mu), v; \mu) = f(v; \mu), \quad \forall v \in \tilde{\mathcal{S}}_A. \quad (31)$$

Here,  $\tilde{\mathcal{S}}_A \subseteq \tilde{\mathcal{S}}$  is defined as in (29) with  $\Phi_{p,k}(\mu)$  replaced by  $\tilde{\Phi}_{p,k}(\mu)$ , and  $\tilde{U}_A$  is hence the solution of an RB-approximated active system  $\tilde{\mathbb{A}}_{AA}(\mu) \tilde{U}_A(\mu) = \tilde{\mathbb{F}}_A(\mu)$ . Note that both  $\tilde{\mathcal{S}}_A$  and  $\mathcal{S}_A$  are subspaces of  $X^h(\Omega)$ , and hence both  $u_A(\mu)$  and  $\tilde{u}_A(\mu)$  are Galerkin-optimal approximations [24] to  $u^h(\mu)$ .

### 3.2 Port Approximation

We discuss here the port approximation framework as well as our particular choice for the port modes  $\chi_{m,j,k}$ . We shall assume for simplicity that all ports are separated by a non-empty non-port and non-Dirichlet boundary segment; if this is not the case, modifications must be made to the procedures below [12].

To begin, we introduce an expansion of the solution to the global system (7) restricted to any local port  $\gamma_{i,j}$  as

$$u^h(\mu)|_{\gamma_{i,j}} = \sum_{k=1}^{\mathcal{N}_{\mathcal{M}(i),j}^\gamma} \mathbb{U}_{\mathcal{G}_i(j),k}(\mu) \chi_{\mathcal{M}(i),j,k}. \quad (32)$$

Port reduction of the system (25) to obtain the smaller system (26) corresponds to an approximation  $u_A(\mu)|_{\gamma_{i,j}} \approx u^h(\mu)|_{\gamma_{i,j}}$  as a truncated expansion

$$u_A(\mu)|_{\gamma_{i,j}} = \sum_{k=1}^{n_{A,i,j}^\gamma} \mathbb{U}_{A,\mathcal{G}_i(j),k}(\mu) \chi_{\mathcal{M}(i),j,k}. \quad (33)$$

To accommodate this truncation without significant loss in accuracy we must develop a set of port modes which provide rapid decrease in the solution coefficients  $\mathbb{U}_{\mathcal{G}_i(j),k}(\mu)$  for any anticipated solution  $u^h(\mu)|_{\gamma_{i,j}}$ . To this end we introduce for port  $j$  on archetype component  $m$  a space  $Y_{m,j}$  of dimension  $y_{m,j}$  as

$$Y_{m,j} = \text{span}\{\rho_{m,j,1}, \dots, \rho_{m,j,y_{m,j}}\}; \quad (34)$$

here the basis functions  $\rho_{m,j,1}, \dots, \rho_{m,j,y_{m,j}}$  are  $L^2(\hat{\gamma}_{m,j})$ -orthonormal *empirical modes* associated with the archetype component port  $\hat{\gamma}_{m,j}$ ; note we shall always choose  $\rho_{m,j,1}$  constant over  $\hat{\gamma}_{m,j}$  for purposes of our *a posteriori* error bound in Section 4. For now we simply assume that these modes exist; we discuss their

construction through a *pairwise training algorithm* in the next subsection. We also introduce the associated  $L^2(\hat{\gamma}_{m,j})$ -orthogonal discrete complement space  $Y_{m,j}^\perp$  of dimension  $\mathcal{N}_{m,j}^\gamma - y_{m,j}$  such that  $P_{m,j}^h = Y_{m,j} \oplus Y_{m,j}^\perp$ .<sup>4</sup>

Next, let  $P_{m,j;0}^h = \{v \in P_{m,j}^h : v|_{\partial\hat{\gamma}_{m,j}} = 0\}$ , and let  $s_{m,j} \in P_{m,j;0}^h$  satisfy<sup>5</sup>

$$\int_{\hat{\gamma}_{m,j}} \nabla s_{m,j} \cdot \nabla v = \int_{\hat{\gamma}_{m,j}} v, \quad \forall v \in P_{m,j;0}^h. \quad (35)$$

Then, we consider a singular Sturm–Liouville eigenvalue problem restricted to the orthogonal complement space  $Y_{m,j}^\perp$ : find pairs  $(\kappa_{m,j}^k, \tau_{m,j}^k) \in \mathbb{R} \times Y_{m,j}^\perp$  such that

$$\int_{\hat{\gamma}_{m,j}} s_{m,j} \nabla \tau_{m,j}^k \cdot \nabla v = \kappa_{m,j}^k \int_{\hat{\gamma}_{m,j}} \tau_{m,j}^k v, \quad \forall v \in Y_{m,j}^\perp, \quad 1 \leq k \leq \mathcal{N}_{m,j}^\gamma - y_{m,j}, \quad (36)$$

with normalization  $\|\tau_{m,j}^k\|_{L^2(\hat{\gamma}_{m,j})} = 1$ ; we order the eigenfunctions according to increasing associated eigenvalue.

We may now identify our port modes and hence our port approximation spaces: we set

$$\chi_{m,j,k} = \begin{cases} \rho_{m,j,k} & 1 \leq k \leq y_{m,j}, \\ \tau_{m,j}^{k-y_{m,j}} & y_{m,j} + 1 \leq k \leq \mathcal{N}_{m,j}^\gamma. \end{cases} \quad (37)$$

Note that the basis functions  $\chi_{m,j,k}$  are  $L^2(\hat{\gamma}_{m,j})$ -orthonormal by construction. On each local port  $j$  on archetype component  $m$ , the  $y_{m,j}$  empirical modes shall be tailored to the family of solutions that we expect on that port for different values of *system* parameters and topology; we introduce an algorithm for the construction of these modes below. The  $\mathcal{N}_{m,j}^\gamma - y_{m,j}$  orthogonal complement eigenmodes complete the discrete space in a well-conditioned fashion.

Note that in the particular case of  $y_{m,j} = 0$  and *one-dimensional* ports our port approximation is of pure Legendre-polynomial type, and we expect (based on classical results for the continuous case  $\mathcal{N}_{m,j}^\gamma \rightarrow \infty$ ) that the eigenmode expansion will exhibit good approximation properties; the port approximation error will decay with an exponential rate with exponent linear in the number of active degrees of freedom — as long as the solution on the port is a (spatially) smooth function [4]. We would not in general expect a similar result for the “classical” non-singular Sturm–Liouville choice  $s_{m,j} = 1$ , and we note that port reduction approaches within the CMS framework [6, 18] typically consider regular rather than singular eigenproblems. Also note that in the case  $y_{m,j} = 0$  a solution to (36) is always  $(\kappa_{m,j}^1 = 0, \tau_{m,j}^1 = \text{constant})$ , and hence  $\chi_{m,j,1}$  is constant for any  $y_{m,j}$  (recall in the case  $y_{m,j} > 0$  we set  $\chi_{m,j,1} = \rho_{m,j,1}$ , which is *chosen* constant).

For *three-dimensional* problems and thus two-dimensional ports, the  $y_{m,j} = 0$  case corresponds to approximation by geometrically generalized Legendre eigenmodes. In this case our approach is conceptually similar to the generalized eigenfunction expansion employed for the approximation of the Navier–Stokes equations in [2]. However for two-dimensional (square, say) ports, the  $y_{m,j} = 0$  approximation would for our purposes here not provide sufficiently rapid error decay. We conjecture in this case that the port approximation error will decay at an exponential rate but with exponent linear in the *square root* of the number of active degrees of freedom. Hence we consider in general  $y_{m,j} > 0$ .

We now consider an approach for generation of the empirical modes in (34) through *pairwise training*. To formalize the procedure we first introduce the (discrete) generalized Legendre polynomials  $L_{m,j}^k \in P_{m,j}^h$  which satisfy the singular Sturm–Liouville eigenproblem

$$\int_{\hat{\gamma}_{m,j}} s_{m,j} \nabla L_{m,j}^k \cdot \nabla v = \Lambda_{m,j}^k \int_{\hat{\gamma}_{m,j}} L_{m,j}^k v, \quad \forall v \in P_{m,j}^h, \quad 1 \leq k \leq \mathcal{N}_{m,j}^\gamma, \quad (38)$$

<sup>4</sup>For a basis function coefficient matrix  $\mathbb{Y} = [\rho_{m,j,1}, \dots, \rho_{m,j,y_{m,j}}] \in \mathbb{R}^{\mathcal{N}_{m,j}^\gamma \times y_{m,j}}$  and an  $L^2(\hat{\gamma}_{m,j})$  inner-product matrix  $\mathbb{X} \in \mathbb{R}^{\mathcal{N}_{m,j}^\gamma \times \mathcal{N}_{m,j}^\gamma}$ , a basis for the orthogonal complement space  $Y_{m,j}^\perp$  is obtained as the  $\mathcal{N}_{m,j}^\gamma - y_{m,j}$  right singular vectors of the matrix  $(\mathbb{X}\mathbb{Y})^T$  which correspond to zero singular values.

<sup>5</sup>Note in (35), and in (36) and (38) below,  $\nabla$  denotes the *surface* gradient operator.

for  $s_{m,j}$  defined in (35). The  $L_{m,j}^k$ , which shall play a role in our empirical mode construction algorithm below, are different from the approximation modes in (36) since (36) is restricted to a *subspace* of  $P_{m,j}^h$ . For our algorithm we shall also require a random variable  $r$  with univariate uniform density over  $(-1, 1)$ , and an algorithm tuning parameter related to anticipated regularity,  $\eta$ .

---

**Algorithm 2** Pairwise training (two components connected at global port  $\Gamma_{p^*}$ )

---

$S_{\text{pair}} = \emptyset$ .

**for**  $n = 1, \dots, N_{\text{samples}}$  **do**

Assign random parameters  $\mu_i \in \mathcal{D}_i$  to component  $i = 1, 2$ .

On all non-shared ports  $\Gamma_p$ ,  $p \neq p^*$ , assign random boundary conditions:

$$u|_{\Gamma_p} = \sum_{k=1}^{\mathcal{N}_{i,j}^\gamma} r \frac{1}{k^\eta} L_{i,j}^k$$

Extract solution  $u|_{\Gamma_{p^*}}$  on shared port.

Add mean-corrected port solution to snapshot set:

$$S_{\text{pair}} \leftarrow S \cup \left( u|_{\Gamma_{p^*}} - \frac{1}{|\Gamma_{p^*}|} \int_{\Gamma_{p^*}} u|_{\Gamma_{p^*}} \right).$$

**end for**

---

To construct the empirical modes we first identify groups of local ports on the archetype components which may interconnect — “port groups;” hence, due to our conformity requirement (9) a, the port space basis functions for all ports in each such port group must be identical. For each pair of local ports within each port group (connected to form a shared global port  $\Gamma_{p^*}$ ), we execute Algorithm 2: we sample this  $I = 2$  component system many ( $N_{\text{samples}}$ ) times for random (typically uniformly or log-uniformly distributed) parameters over the parameter domain and for random boundary conditions on non-shared ports; note that the enforced coefficient decay in the boundary condition expansion ( $\eta > 1$ ) ensures in particular that the boundary conditions are  $L^2(\Gamma_p)$  functions. For each sample we extract the solution on the shared port  $\Gamma_{p^*}$ ; we then subtract its average and add the resulting zero-mean function to a snapshot set  $S_{\text{pair}}$ . Note that by construction all functions in  $S_{\text{pair}}$  are thus orthogonal to the constant function.

Upon completion of Algorithm 2 for all possible component connectivities within a port group, we next form a larger snapshot set  $S_{\text{group}}$  which is the union of all the snapshot sets  $S_{\text{pair}}$  generated for each pair.<sup>6</sup> We then perform a data compression step: we invoke the proper orthogonal decomposition (POD) [19] (with respect to the  $L^2(\Gamma_{p^*})$  inner product). The output from the POD procedure is a set of  $y_{m,j} - 1$  mutually  $L^2(\Gamma_{p^*})$ -orthonormal empirical modes which have the additional property that they are orthogonal to the constant function over  $\Gamma_{p^*}$ . For each archetype component and local port pair  $(m, j)$  in each port group we assign the port space basis functions in (37) as follows: we first assign the (normalized) constant to  $\rho_{m,j,1}$ ; we then assign the  $y_{m,j} - 1$  first POD modes to  $\rho_{m,j,k}$ ,  $2 \leq k \leq y_{m,j}$ ; the remaining port modes  $\tau_{m,j}^k$ ,  $1 \leq k \leq \mathcal{N}_{m,j}^\gamma - y_{m,j}$ , are then defined from (34) and (36). Finally, we repeat the procedure for all port groups in the library of archetype components.

In the case that ports are not separated by a non-Dirichlet, non-port boundary segment, we must make some adjustments to the procedures above. In the case in which ports are not separated by a non-port segment (ports “touch” at a point) we enforce zero Dirichlet conditions in (36) *and* we require an additional special port mode which couples the two ports; furthermore we do *not* explicitly include the constant function as  $\rho_{m,j,1}$  in our port space basis. We note that such component connectivity is considered in [12] in the CMS context. In the case that ports are separated by a zero Dirichlet non-port boundary segment we simply

---

<sup>6</sup>We must technically map the snapshots to a common domain associated with the port group; however we omit this step here to avoid cumbersome notation.

enforce the Dirichlet conditions on the port modes directly in the eigenproblem (36); we must also make adjustments to our empirical training algorithm to make sure that the resulting POD modes are also zero on the boundary of the port.

## 4 A *Posteriori* Error Bound

We shall develop here an *a posteriori* bound for the error  $e^h(\mu) \equiv u^h(\mu) - u_A(\mu)$  associated with our port-reduced static condensation approximation. In the first subsection we introduce relevant notation and discuss the norms and outputs for which we develop our bounds. In actual practice, when we employ the SCRBE for bubble function approximation, our error bounds must of course reflect RB errors in the bubble functions; we consider these additional RB contributions to the error bounds in Appendix A.

### 4.1 Preliminaries: Norms and Outputs

We shall develop a bound for the error measured in the usual (global) energy norm

$$\|\omega\|_\mu \equiv \sqrt{a(\omega, \omega; \mu)}, \quad \forall \omega \in H^1(\Omega), \quad (39)$$

which thanks to coercivity and continuity of  $a(\cdot, \cdot; \mu)$  is equivalent to the standard  $H^1(\Omega)$ -norm. We also introduce the ‘‘Schur energy norm’’ given by

$$\|v\|_{\mathbb{A}(\mu)} \equiv \sqrt{v^T \mathbb{A}(\mu) v}, \quad \forall v \in \mathbb{R}^{n_{sc}}, \quad (40)$$

which shall serve as an ingredient in our error bound derivation. We note that for any function  $\omega(\mu) = \sum_{p=1}^{n^\Gamma} \sum_{k=1}^{N_p^\Gamma} v_{p,k} \Phi_{p,k}(\mu)$ ,  $\omega(\mu) \in \mathcal{S}$ , and it thus follows directly from the definition of  $\mathbb{A}(\mu)$  in (17) that

$$\|v\|_{\mathbb{A}(\mu)}^2 = a(\omega, \omega; \mu). \quad (41)$$

This relation connects an algebraic Schur complement to our partial differential equation.

The solution to our port-reduced problem (in the absence of RB errors) is the vector  $\mathbb{U}_A(\mu)$  in (26). We extend this vector as

$$\hat{\mathbb{U}}_A(\mu) \equiv \begin{bmatrix} \mathbb{U}_A(\mu) \\ \mathbf{0} \end{bmatrix} \in \mathbb{R}^{n_{sc}}, \quad (42)$$

such that  $\hat{\mathbb{U}}_A(\mu)$  is zero for all entries that correspond to inactive port modes. We then define the error vector associated with the port-reduced approximation as

$$\mathbb{E}(\mu) \equiv \mathbb{U}(\mu) - \hat{\mathbb{U}}_A(\mu) \in \mathbb{R}^{n_{sc}}; \quad (43)$$

the associated error in the field is, from (14) and (27),

$$e^h(\mu) = u^h(\mu) - u_A(\mu) = \sum_{p=1}^{n^\Gamma} \sum_{k=1}^{N_p^\Gamma} \mathbb{E}_{p,k}(\mu) \Phi_{p,k}(\mu); \quad (44)$$

note that  $e^h(\mu) \in \mathcal{S}$  because of cancellation of the bubbles  $\sum_{i=1}^I b_i^{f;h}(\mu_i)$  associated with the right-hand side. Note if the SCRBE is employed, the solution to our port-reduced problem is  $\tilde{\mathbb{U}}_A(\mu)$ , and hence in actual practice  $\mathbb{E}(\mu) = \mathbb{U}(\mu) - \hat{\tilde{\mathbb{U}}}_A(\mu)$ , where  $\hat{\tilde{\mathbb{U}}}_A(\mu)$  is a zero-extended version of  $\tilde{\mathbb{U}}_A(\mu)$ ; note that the associated error in the field  $e^h(\mu) = u^h(\mu) - \tilde{u}_A(\mu)$  is no longer in  $\mathcal{S}$  due to the RB approximations (20).

It follows from (44) and (41) that, in the absence of RB errors,  $\|\mathbb{E}(\mu)\|_{\mathbb{A}(\mu)} = \|e^h(\mu)\|_\mu$  and hence a bound on the error in the Schur energy norm is also a bound on the energy of the error in the field. Furthermore,

even in the presence of (small) RB errors,  $e^h(\mu)$  is “almost” in  $\mathcal{S}$  and thus the Schur energy norm remains relevant. For this reason we shall pursue a bound for the error in the Schur energy norm first — here, in the body of the paper — in the absence of RB errors which we shall subsequently modify — in Appendix A — to obtain a bound on the energy  $\|e^h(\mu)\|_\mu$  valid even in the presence of RB errors.

We shall also develop bounds for derived quantities defined over the ports. For any particular global port  $\Gamma_{p^*}$  we introduce a (parameter independent) bounded output functional  $\ell^{\Gamma_{p^*}}(\cdot) : L^2(\Gamma_{p^*}) \rightarrow \mathbb{R}$ ; we then define our FE output of interest as

$$s^h(\mu) = \ell^{\Gamma_{p^*}}(u^h(\mu)|_{\Gamma_{p^*}}), \quad (45)$$

which from (14) can be written as

$$s^h(\mu) = \sum_{k=1}^{\mathcal{N}_p^\Gamma} \mathbb{U}_{p^*,k}(\mu) \ell^{\Gamma_{p^*}}(\Psi_{p^*,k}) \quad (46)$$

since  $u^h(\mu)|_{\Gamma_{p^*}} = \mathbb{U}_{p^*,k}(\mu) \Psi_{p^*,k}|_{\Gamma_{p^*}}$  (note we henceforth take the restriction to  $\Gamma_{p^*}$  of arguments to  $\ell^{\Gamma_{p^*}}$  as understood). We may also write this output as

$$s^h(\mu) = \mathbb{L}(\mu)^\top \mathbb{U}(\mu), \quad (47)$$

where  $\mathbb{L}(\mu) \in \mathbb{R}^{n_{\text{sc}}}$  is defined as  $\mathbb{L}_{p,k}(\mu) = \ell^{\Gamma_p}(\Psi_{p,k})$  for  $p = p^*$  and as  $\mathbb{L}_{p,k}(\mu) = 0$  for  $p \neq p^*$ . We define the port-reduced output approximation as

$$s_A(\mu) \equiv \ell^{\Gamma_{p^*}}(u_A(\mu)) = \mathbb{L}(\mu)^\top \hat{\mathbb{U}}_A(\mu). \quad (48)$$

We again recall that  $e^h(\mu) \in \mathcal{S}$  in the absence of RB error, and thus for the output error we may obtain a bound as

$$|s^h(\mu) - s_A(\mu)| = |\ell^{\Gamma_{p^*}}(u^h(\mu)|_{\Gamma_{p^*}} - u_A(\mu)|_{\Gamma_{p^*}})| \leq \|e^h(\mu)\|_\mu \sup_{v \in \mathcal{S}} \frac{\ell^{\Gamma_{p^*}}(v)}{\|v\|_\mu}, \quad (49)$$

The term  $\sup_{v \in \mathcal{S}} \frac{\ell^{\Gamma_{p^*}}(v)}{\|v\|_\mu}$  is efficiently boundable — we provide a comment in Remark 3 of Section 4.5 once the necessary tools are introduced. If the SCRBE is employed  $e^h(\mu)$  is no longer a member of  $\mathcal{S}$ , and hence a modification to (49) is necessary; however we do not consider this modification to (49) in the current paper.

Although the theory (and associated computational procedures) in the next sections extends also to the case of non-compliance [23, 25] outputs (as indicated by (49)), and for outputs which are not defined over ports [15], we shall for our numerical results in this paper restrict attention to the case of compliance port outputs. For example, if  $f(v; \mu) = f(v)$  corresponds to a (parameter-independent) uniform external load on  $\Gamma_{p^*}$ , the compliance output  $\ell_{\Gamma_{p^*}}(v) = f(v)$  is the integrated (or average) field variable over  $\Gamma_{p^*}$ . Note that the port restriction on  $f(v)$  implies  $b_i^{f;h}(\mu_i) = 0$ ,  $1 \leq i \leq I$ , in (12), and thus  $u_A(\mu) \in \mathcal{S}_A$ . For compliance port outputs we readily obtain in this case the standard result

$$s^h(\mu) - s_A(\mu) = \|e^h(\mu)\|_\mu^2, \quad (50)$$

thanks to Galerkin orthogonality of  $e^h(\mu)$  with respect to  $\mathcal{S}_A \subset X^h(\Omega)$  and symmetry and coercivity of  $a(\cdot, \cdot; \mu)$ .

In the remainder of this section we focus on the Schur energy norm error bound in the absence of RB errors; RB errors are accounted for in Appendix A for the energy error in the field and for error in compliance outputs. We begin our error bound development with an exact variational error statement and then introduce two relaxation steps — a non-conforming approximation and an error bound conditioner — that in tandem significantly reduce the cost of the error bound computation while maintaining sufficient sharpness. We first consider the theoretical approximation aspects and then the computational aspects.

## 4.2 Exact Variational Error Statement

The residual associated with the port-reduced static condensation approximation is

$$\mathbb{R}(\mu) \equiv \mathbb{F}(\mu) - \mathbb{A}(\mu)\hat{\mathbb{U}}_{\mathbb{A}}(\mu). \quad (51)$$

We note that since  $\mathbb{F}(\mu) = \mathbb{A}(\mu)\mathbb{U}(\mu)$  we directly obtain the usual error-residual relationship

$$\mathbb{A}(\mu)\mathbb{E}(\mu) = \mathbb{R}(\mu); \quad (52)$$

since  $\mathbb{A}(\mu)$  is an SPD matrix we also have [26]

$$\mathbb{E}(\mu) = \arg \min_{v \in \mathbb{R}^{n_{\text{SC}}}} \mathcal{J}(v; \mu), \quad (53)$$

where  $\mathcal{J}(\cdot; \mu)$  is the quadratic functional given by

$$\mathcal{J}(v; \mu) \equiv \frac{1}{2}v^{\text{T}}\mathbb{A}(\mu)v - v^{\text{T}}\mathbb{R}(\mu), \quad \forall v \in \mathbb{R}^{n_{\text{SC}}}. \quad (54)$$

For the error in the system solution in the Schur energy norm we then obtain

$$\|\mathbb{E}(\mu)\|_{\mathbb{A}(\mu)}^2 = \mathbb{E}(\mu)^{\text{T}}\mathbb{A}(\mu)\mathbb{E}(\mu) = \mathbb{R}(\mu)^{\text{T}}\mathbb{E}(\mu) = -2\mathcal{J}(\mathbb{E}(\mu); \mu) \quad (55)$$

(note that  $\mathcal{J}(\mathbb{E}(\mu); \mu)$  is *negative*).

## 4.3 Step 1: Non-Conforming Error Approximation

The first ingredient in our *a posteriori* error bound is a non-conforming approximation to  $\mathbb{E}(\mu)$ . We start with the Schur complement matrix  $\mathbb{A}(\mu) \in \mathbb{R}^{n_{\text{SC}} \times n_{\text{SC}}}$  and residual vector  $\mathbb{R}(\mu) \in \mathbb{R}^{n_{\text{SC}}}$ . We consider the full system, but with  $n_{\text{A}}$  degrees of freedom marked as active, and  $n_{\text{I}}$  degrees of freedom marked as inactive. We then introduce an expanded non-conforming system with  $n'_{\text{SC}} = n_{\text{SC}} + n'_{\text{I}}$  degrees of freedom, where  $n'_{\text{I}}$  is the number of inactive degrees of freedom associated with *shared* global ports.

We first define a constraint matrix  $C \in \mathbb{R}^{n'_{\text{I}} \times n'_{\text{SC}}}$  and a matrix  $D \in \mathbb{R}^{n'_{\text{SC}} \times n_{\text{SC}}}$  such that  $\ker(C)$  is spanned by the columns of  $D$ . The expanded dimension  $n'_{\text{SC}}$  corresponds to duplication of the  $n'_{\text{I}}$  inactive degrees of freedom associated with shared ports; the constraint matrix  $C$  corresponds to equality constraints imposed on these degrees of freedom. We note that  $n_{\text{SC}} = \text{rank}(D)$  and hence

$$\forall w' \in \ker(C), \text{ there exists a unique } w \in \mathbb{R}^{n_{\text{SC}}} \text{ such that } w' = Dw. \quad (56)$$

We then introduce an expanded stiffness matrix and residual vector  $\mathbb{A}'(\mu) \in \mathbb{R}^{n'_{\text{SC}} \times n'_{\text{SC}}}$  and  $\mathbb{R}'(\mu) \in \mathbb{R}^{n'_{\text{SC}}}$  such that the relations

$$\mathbb{A}(\mu) = D^{\text{T}}\mathbb{A}'(\mu)D \in \mathbb{R}^{n_{\text{SC}} \times n_{\text{SC}}}, \quad \mathbb{R}(\mu) = D^{\text{T}}\mathbb{R}'(\mu) \in \mathbb{R}^{n_{\text{SC}}}, \quad (57)$$

hold. For our expanded matrix  $\mathbb{A}'(\mu)$  we then state

**Conjecture 1.** *Assume that  $n_{\text{A},p}^{\Gamma} \geq 1$  for  $1 \leq p \leq n^{\Gamma}$ . Then the symmetric matrix  $\mathbb{A}'(\mu)$  is positive definite.*

*Sketch of proof.* We consider the Laplace equation in a two-component system with component domains  $\Omega_1$  and  $\Omega_2$  such that  $a(w, v) = \sum_{i=1}^2 \int_{\Omega_i} \nabla w \cdot \nabla v$  for  $w, v \in H^1(\Omega_i)$ ,  $i = 1, 2$ . The components are connected at a single global port  $\Gamma_1$  and we associate to this port (and thus system)  $n_{\text{A},1}^{\Gamma} = n_{\text{A}} \geq 1$  active degrees of freedom. To ensure well-posedness of (6) in this case, we assume homogeneous Dirichlet boundary conditions on a non-empty subset of the non-port boundary of  $\Omega_1$ ; on all other boundaries of the system we consider homogeneous Neumann conditions.

To any  $v \in \mathbb{R}^{n'_{\text{sc}}}$  we associate a function  $w \equiv w_{\text{A}} + w_{\text{I},1} + w_{\text{I},2}$  such that

$$w_{\text{A}} \equiv \sum_{k=1}^{n_{\text{A}}} v_k \Phi_{1,k}, \quad (58)$$

and

$$w_{\text{I},1} \equiv \sum_{k=n_{\text{A}}+1}^{n_{\text{A}}+n_{\text{I}}} v_k \Phi_{1,k}|_{\Omega_1}, \quad w_{\text{I},2} \equiv \sum_{k=n_{\text{A}}+1}^{n_{\text{A}}+n_{\text{I}}} v_{n_1+k} \Phi_{1,k}|_{\Omega_2}; \quad (59)$$

note that  $w$  is discontinuous over  $\Gamma_1$  and that  $w_{\text{I},1}$  and  $w_{\text{I},2}$  are defined over  $\Omega_1$  and  $\Omega_2$ , respectively. With  $\mathbb{A}'$  expanded from  $\mathbb{A}$  (for  $a(\cdot, \cdot; \mu)$  defined in (4)) we obtain

$$\begin{aligned} v^{\text{T}} \mathbb{A}' v &= a_1(w_{\text{A}}|_{\Omega_1} + w_{\text{I},1}, w_{\text{A}}|_{\Omega_1} + w_{\text{I},1}) \\ &\quad + a_2(w_{\text{A}}|_{\Omega_2} + w_{\text{I},2}, w_{\text{A}}|_{\Omega_2} + w_{\text{I},2}) \\ &= |w_{\text{A}}|_{\Omega_1} + w_{\text{I},1}|_{H^1(\Omega_1)}^2 + |w_{\text{A}}|_{\Omega_2} + w_{\text{I},2}|_{H^1(\Omega_2)}^2 \geq 0; \quad (60) \end{aligned}$$

here,  $|\cdot|_{H^1(\Omega_i)}$  denotes the  $H^1(\Omega_i)$  semi-norm. Thus if  $v^{\text{T}} \mathbb{A}' v = 0$ , we must have  $w_{\text{A}} + w_{\text{I},i} = c_i$ ,  $i = 1, 2$ , for constants  $c_1, c_2$ . Since  $n_{\text{A},p}^{\Gamma} \geq 1$ , the set of active port modes on  $\Gamma_1$  contains at least the constant mode. As all modes except this first mode have zero mean on  $\Gamma_1$  (per Algorithm 2), and as these modes are linearly independent, we must have  $v_k = 0$  for all  $k > 1$ . Thus, in particular,  $w_{\text{I},1} = w_{\text{I},2} = 0$ , and as a result  $w = w_{\text{A}} = v_1 \Phi_{1,1} = c_1 = c_2$ . But as we consider homogeneous Dirichlet conditions on parts of the boundary of  $\Omega_1$ , we must have  $v_1 \Phi_{1,1} = c_1 = c_2 = 0$  and thus also  $v_k = 0$  for all  $k$  since  $\Phi_{1,1}$  is non-zero.  $\square$

We believe that in the more general case a Poincaré-Friedrichs inequality will serve to demonstrate invertibility of  $\mathbb{A}'(\mu)$ .

We then define an associated “expanded” functional  $\mathcal{J}'(\cdot; \mu) : \mathbb{R}^{n'_{\text{sc}}} \rightarrow \mathbb{R}$  as

$$\mathcal{J}'(v; \mu) = \frac{1}{2} v^{\text{T}} \mathbb{A}'(\mu) v - v^{\text{T}} \mathbb{R}'(\mu). \quad (61)$$

We now consider the minimum of  $\mathcal{J}'(\cdot; \mu)$  over  $\ker(C) \subset \mathbb{R}^{n'_{\text{sc}}}$ , denoted

$$\mathbb{E}'_C(\mu) \equiv \arg \min_{v \in \ker(C)} \mathcal{J}'(v; \mu). \quad (62)$$

We observe that (62) is merely a restatement of (53) over a constrained space of dimension  $n_{\text{SC}}$  embedded in  $\mathbb{R}^{n'_{\text{sc}}}$ : from (56) and (57) we may conclude that  $\mathcal{J}(\mathbb{E}(\mu); \mu) = \mathcal{J}'(\mathbb{E}'_C(\mu); \mu)$  with  $\mathbb{E}'_C(\mu) = D\mathbb{E}(\mu)$ .

We next remove the constraints and consider minimization of  $\mathcal{J}'(\cdot; \mu)$  over  $\mathbb{R}^{n'_{\text{sc}}}$ . In particular, we then define

$$\mathbb{E}'(\mu) \equiv \arg \min_{v \in \mathbb{R}^{n'_{\text{sc}}}} \mathcal{J}'(v; \mu). \quad (63)$$

It follows from the associated Euler equation that  $\mathbb{E}'(\mu) = \mathbb{A}'(\mu)^{-1} \mathbb{R}'(\mu)$  (recall that  $\mathbb{A}'(\mu)$  is invertible by Conjecture 1). We may then state

**Lemma 1.** *The error in the Schur energy norm is bounded as*

$$\|\mathbb{E}(\mu)\|_{\mathbb{A}(\mu)}^2 \leq -2\mathcal{J}'(\mathbb{E}'(\mu); \mu). \quad (64)$$

*Proof.* Since the minimization in (63) is taken over a larger space than the minimization in (62), we obtain

$$\mathcal{J}'(\mathbb{E}'(\mu); \mu) \leq \mathcal{J}'(\mathbb{E}'_C(\mu); \mu). \quad (65)$$

The result (64) then follows from  $\mathcal{J}'(\mathbb{E}'_C(\mu); \mu) = \mathcal{J}(\mathbb{E}(\mu); \mu)$  and (55).  $\square$



**Remark 2.** We note that the field variable  $(e^h)'(\mu)$  associated with  $\mathbb{E}'(\mu)$  is indeed a non-conforming approximation to the field variable  $e^h(\mu)$ ; note that  $(e^h)'(\mu) \in X'(\Omega)$  for  $X'(\Omega) \supset X^h(\Omega)$  due to the discontinuities across shared global ports, and note that the associated “jumps” may be represented exactly by the  $n_{\Gamma_p}^{\Gamma}$  “highest order” modes at each port  $\Gamma_p$ .

A full analysis of this non-conforming approximation necessitates a functional formulation which we do not consider here. However, we note that the approximation and consistency contribution to the error (in the error approximation) may be analyzed and bounded through Strang’s Second Lemma [8]. In particular, in [5, Eq. 18], the consistency error is written as a boundary integral of the normal derivative of the exact error multiplied by jump terms,

$$\sup_{w \in X'(\Omega)} \int_{\cup_{p=1}^n \Gamma_p} \frac{\partial_n e^h[w]}{\|w\|}, \quad (66)$$

where  $[w]$  denotes the jump associated with  $w$  at a particular port and  $\|\cdot\|$  here is a broken  $H^1(\Omega)$ -norm. We thus expect the consistency error term to be very small if  $\partial_n e^h$  can be well represented by the basis functions associated with the low-order (active) modes, which are perforce  $L^2$ -orthogonal to  $[w]$ ; and we furthermore expect  $\partial_n e^h$  to be relatively low order if our port approximation procedure provides an effective port expansion (for  $u^h(\mu)$ ).

#### 4.4 Step 2: Error Bound Conditioner

The second ingredient in our error upper bound is a parameter-independent bound conditioner. As our conditioner we consider a reference system Schur complement matrix, that is

$$\mathbb{B} = \mathbb{A}(\mu_{\text{ref}}), \quad (67)$$

where  $\mu_{\text{ref}} \in \mathcal{D}$  is a reference parameter value. We introduce an associated expanded reference matrix  $\mathbb{B}' \in \mathbb{R}^{n'_{\text{sc}} \times n'_{\text{sc}}}$  such that  $\mathbb{B} = D^T \mathbb{B}' D$ . Recall that  $\mathbb{B}'(\mu) = \mathbb{A}'(\mu_{\text{ref}})$  is invertible by Conjecture 1.

We then introduce the generalized eigenproblem associated with  $\mathbb{B}'$  and  $\mathbb{A}'(\mu)$ ,

$$\mathbb{A}'(\mu)v_i(\mu) = \lambda_i(\mu)\mathbb{B}'v_i, \quad 1 \leq i \leq n'_{\text{sc}}. \quad (68)$$

We denote by  $\lambda_{\min}(\mu) \equiv \lambda_1(\mu)$  the smallest eigenvalue associated with (68); hence

$$\lambda_{\min}(\mu)v^T \mathbb{B}'v \leq v^T \mathbb{A}'(\mu)v, \quad \forall v \in \mathbb{R}^{n'_{\text{sc}}}. \quad (69)$$

We may then introduce a modified functional  $\mathcal{J}'_{\mathbb{B}}(\cdot; \mu) : \mathbb{R}^{n'_{\text{sc}}} \rightarrow \mathbb{R}$  as

$$\mathcal{J}'_{\mathbb{B}}(v; \mu) = \frac{\lambda_{\min}(\mu)}{2} v^T \mathbb{B}'v - v^T \mathbb{R}'(\mu), \quad (70)$$

for which, for any  $v \in \mathbb{R}^{n'_{\text{sc}}}$ ,

$$\mathcal{J}'_{\mathbb{B}}(v; \mu) \leq \mathcal{J}'(v; \mu). \quad (71)$$

We now define

$$\mathbb{E}'_{\mathbb{B}}(\mu) \equiv \arg \min_{v \in \mathbb{R}^{n'_{\text{sc}}}} \mathcal{J}'_{\mathbb{B}}(v; \mu), \quad (72)$$

and note that

$$\mathbb{E}'_{\mathbb{B}}(\mu) \equiv \frac{1}{\lambda_{\min}(\mu)} (\mathbb{B}')^{-1} \mathbb{R}'(\mu) \quad (73)$$

from the Euler-Lagrange equation associated with (72).

We are now ready to formulate

**Lemma 2.** *The error in the Schur energy norm is bounded as*

$$\|\mathbb{E}(\mu)\|_{\mathbb{A}(\mu)}^2 \leq -2\mathcal{J}'_{\mathbb{B}}(\mathbb{E}'_{\mathbb{B}}(\mu); \mu) = \frac{\mathbb{R}'(\mu)^{\text{T}}(\mu)(\mathbb{B}')^{-1}\mathbb{R}'(\mu)}{\lambda_{\min}(\mu)} \quad (74)$$

*Proof.* From (72) and (69), we first obtain

$$\mathcal{J}'_{\mathbb{B}}(\mathbb{E}'_{\mathbb{B}}(\mu); \mu) \leq \mathcal{J}'_{\mathbb{B}}(\mathbb{E}'(\mu); \mu) \leq \mathcal{J}'(\mathbb{E}'(\mu); \mu). \quad (75)$$

The inequality in (74) then follows from Lemma 1. The equality in (74) follows from (73) and (70).  $\square$

In the context of port reduction it is not desirable to calculate the eigenvalue  $\lambda_{\min}(\mu)$  as this would require formation of the entire matrix  $\mathbb{A}'(\mu)$  and solution of the expanded generalized eigenproblem (68). We instead pursue an eigenvalue *lower bound* through an *eigenproblem residual* (a similar procedure is demonstrated in [17] for the standard eigenproblem). To this end, we first introduce the eigenproblem associated with the  $n_{\text{A}}$  active degrees of freedom as

$$\mathbb{A}_{\text{AA}}(\mu)v_{\text{A},i}(\mu) = \lambda_{\text{A},i}(\mu)\mathbb{B}_{\text{AA}}v_{\text{A},i}(\mu), \quad v_{\text{A},i}^{\text{T}}\mathbb{B}_{\text{AA}}v_{\text{A},i} = 1, \quad (76)$$

for  $1 \leq i \leq n_{\text{A}}$ . We denote by  $\lambda_{\text{A},\min}(\mu) \equiv \lambda_{\text{A},1}(\mu)$  the smallest eigenvalue associated with (76). We introduce an extended associated eigenvector

$$\hat{v}_{\text{A},1}(\mu) = \begin{bmatrix} v_{\text{A},1}(\mu) \\ \mathbf{0} \end{bmatrix} \in \mathbb{R}^{n'_{\text{SC}}}. \quad (77)$$

With the two eigenproblems (76) and (68) we may then define the eigenproblem residual

$$\mathbb{R}'_{\text{eig}}(\mu) \equiv \mathbb{A}'(\mu)\hat{v}_{\text{A},1}(\mu) - \lambda_{\text{A},\min}(\mu)\mathbb{B}'\hat{v}_{\text{A},1}(\mu). \quad (78)$$

(Note that as only the inactive degrees of freedom are duplicated in the expanded system, we interpret  $\mathbb{A}_{\text{AA}}(\mu)$  and  $\mathbb{B}_{\text{AA}}$  as the upper left submatrices of  $\mathbb{A}'$  and  $\mathbb{B}'$ , respectively.)

We now state

**Proposition 1.** *For any  $\mu \in \mathcal{D}$  let*

$$\lambda_{\min,\text{LB}}(\mu) \equiv \lambda_{\text{A},\min}(\mu) - \sqrt{\mathbb{R}'_{\text{eig}}(\mu)^{\text{T}}(\mathbb{B}')^{-1}\mathbb{R}'_{\text{eig}}(\mu)}. \quad (79)$$

*Further, assume that*

$$|\lambda_{\text{A},\min}(\mu) - \lambda_{\min}(\mu)| \leq |\lambda_{\text{A},\min}(\mu) - \lambda_i(\mu)|, \quad 1 \leq i \leq n'_{\text{SC}}. \quad (80)$$

*Then*

$$\lambda_{\min,\text{LB}}(\mu) \leq \lambda_{\min}(\mu). \quad (81)$$

*Proof.* We first expand  $\hat{v}_{\text{A},1}$  in terms of the eigenfunctions  $v_i$  of the full eigenproblem (68) as

$$\hat{v}_{\text{A},1} = \sum_{i=1}^{n'_{\text{SC}}} \alpha_i v_i. \quad (82)$$

We note that thanks to the normalization in (76) we also obtain  $\hat{v}_{\text{A},1}^{\text{T}}\mathbb{B}'\hat{v}_{\text{A},1} = 1$ . We consider the ‘‘dual Schur reference norm’’ of the eigenproblem residual as

$$\|\mathbb{R}'_{\text{eig}}\|_{(\mathbb{B}')^{-1}}^2 = \mathbb{R}'_{\text{eig}}(\mu)^{\text{T}}(\mathbb{B}')^{-1}\mathbb{R}'_{\text{eig}}(\mu), \quad (83)$$

for which we obtain from (78) (we omit here all  $\mu$ -dependence for simplicity)

$$\|\mathbb{A}'\hat{v}_{A,1} - \lambda_{A,\min}\mathbb{B}'\hat{v}_{A,1}\|_{(\mathbb{B}')^{-1}}^2 = \left\| \sum_{i=1}^{n'_{\text{SC}}} \alpha_i \mathbb{A}' v_i - \lambda_{A,\min} \sum_{i=1}^{n'_{\text{SC}}} \alpha_i \mathbb{B}' v_i \right\|_{(\mathbb{B}')^{-1}}^2 \quad (84)$$

$$= \left\| \sum_{i=1}^{n'_{\text{SC}}} (\lambda_i - \lambda_{A,\min}) \alpha_i \mathbb{B}' v_i \right\|_{(\mathbb{B}')^{-1}}^2 \quad (85)$$

$$= \sum_{i=1}^{n'_{\text{SC}}} |\lambda_i - \lambda_{A,\min}|^2 \|\alpha_i \mathbb{B}' v_i\|_{(\mathbb{B}')^{-1}}^2 \quad (86)$$

$$\geq |\lambda_{\min} - \lambda_{A,\min}|^2 \sum_{i=1}^{n'_{\text{SC}}} \|\alpha_i \mathbb{B}' v_i\|_{(\mathbb{B}')^{-1}}^2 \quad (87)$$

$$= |\lambda_{\min} - \lambda_{A,\min}|^2 \left\| \sum_{i=1}^{n'_{\text{SC}}} \alpha_i \mathbb{B}' v_i \right\|_{(\mathbb{B}')^{-1}}^2 \quad (88)$$

$$= |\lambda_{\min} - \lambda_{A,\min}|^2. \quad (89)$$

In this derivation, (86) follows from the  $\mathbb{B}'$ -orthogonality of the  $v_i$ , (87) follows from (80), (88) follows from  $\mathbb{B}'$ -orthogonality of the  $v_i$ , and finally (89) follows from the normalization condition on  $\hat{v}_{A,1}$ . We thus conclude that

$$\lambda_{\min,\text{LB}}(\mu) = \lambda_{A,\min}(\mu) - \sqrt{\mathbb{R}'_{\text{eig}}(\mu)^{\text{T}} (\mathbb{B}')^{-1} \mathbb{R}'_{\text{eig}}(\mu)} \quad (90)$$

satisfies  $\lambda_{\min,\text{LB}}(\mu) \leq \lambda_{\min}(\mu)$ .  $\square$

The eigenvalue proximity assumption (80) is the one caveat in our *a posteriori* error bound procedure. We provide computational results in Section 6 that confirm plausibility of this assumption. However, in actual computational practice it remains an unverified assumption. A mitigating consideration is the proximity (typically) of  $\lambda_{\min}(\mu)$  (and  $\lambda_{\min,\text{LB}}(\mu)$ ) to unity such that in any event the effect on the total error bound (of the next section) is small.

Finally, we note that in [29] a similar bound conditioner idea is employed for *reduced basis* approximations. In [29] a multi-reference-parameter approach is also introduced: for a given  $\mu$  an interpolation between a few inverse reference operators is performed to optimize the conditioner. We expect that a multi-reference-parameter approach is applicable also to our port-reduction error bound conditioner here, but we do not consider this possibility further in the current paper.

## 4.5 A Posteriori Error Bound

Armed with the non-conforming error approximation, the bound conditioner, and the eigenvalue lower bound, we are now ready to state our *a posteriori* error bound result for the port-reduced static condensation approximation in

**Proposition 2.** *Let*

$$\Delta^u(\mu) \equiv \sqrt{\frac{\mathbb{R}'(\mu)^{\text{T}} (\mathbb{B}')^{-1} \mathbb{R}'(\mu)}{\lambda_{\min,\text{LB}}(\mu)}}, \quad (91)$$

and assume that the eigenvalue proximity assumption (80) holds. Then for any  $\mu \in \mathcal{D}$

$$\|u^h(\mu) - u_A(\mu)\|^2 \leq \Delta^u(\mu). \quad (92)$$

*Proof.* We obtain the desired result directly from the definition of  $e^h(\mu)$  in (44) together with (41) and  $e^h(\mu) \in \mathcal{S}$  (per (44)), Lemma 2, and Proposition 1.  $\square$

We also give bounds on the error in the port-reduced port-restricted compliance output quantity  $s_A(\mu) = f(u_A(\mu))$  in

**Corollary 1.** *For the compliance output  $s_A(\mu)$  defined in (48), the output error  $s(\mu) - s_A(\mu)$  satisfies*

$$0 \leq s(\mu) - s_A(\mu) \leq (\Delta^u(\mu))^2; \quad (93)$$

*equivalently, the true output  $s^h(\mu)$  satisfies*

$$s_A(\mu) \leq s^h(\mu) \leq (\Delta^u(\mu))^2 + s_A(\mu). \quad (94)$$

*Proof.* The result follows from (50) and Proposition 2.  $\square$

We consider non-compliance outputs in

**Remark 3.** *To efficiently bound the right-hand side of (49) we now note that*

$$\sup_{\omega \in \mathcal{S}} \frac{\ell^{\Gamma_p^*}(\omega)}{\|\omega\|_\mu} = \sup_{v \in \mathbb{R}^{n_{\text{SC}}}} \frac{\mathbb{L}^T v}{v^T \mathbb{A}(\mu) v} \leq \sup_{v \in \mathbb{R}^{n'_{\text{SC}}}} \frac{(\mathbb{L}')^T v}{v^T \mathbb{A}'(\mu) v} \leq \frac{1}{\lambda_{\min, \text{LB}}(\mu)} \sup_{v \in \mathbb{R}^{n'_{\text{SC}}}} \frac{(\mathbb{L}')^T v}{v^T \mathbb{B}'(\mu) v}. \quad (95)$$

*This bound is efficiently computable: we need only invoke our eigenvalue lower bound  $\lambda_{\min, \text{LB}}(\mu)$ , and perform one additional non-conforming  $\mathbb{B}'$ -solve to compute the supremizer (note we consider here parameter-independent  $\mathbb{L} = \mathbb{L}(\mu)$ ). A bound for the error in port-restricted non-compliance outputs is thus*

$$|s^h(\mu) - s_A(\mu)| \leq \frac{\Delta^u(\mu)}{\lambda_{\min, \text{LB}}(\mu)} \sup_{v \in \mathbb{R}^{n'_{\text{SC}}}} \frac{(\mathbb{L}')^T v}{v^T \mathbb{B}'(\mu) v}. \quad (96)$$

Note in the remainder of this paper we restrict attention to compliance outputs.

An alternative and more straightforward *a posteriori* error bound can be obtained from (52) and the Cauchy–Schwarz inequality as  $\|\mathbb{E}(\mu)\|_2 \leq \|\mathbb{A}(\mu)^{-1}\|_2 \|\mathbb{R}(\mu)\|_2$ . We emphasize that Lemma 2 and Proposition 2 differ from this bound based on direct residual evaluation *not* only because of the different (Schur energy) norm, but also since  $\mathbb{E}'_{\mathbb{B}}(\mu)$  constitutes an approximate *solution* to (52) and hence we do not lose sharpness due to application of the Cauchy–Schwarz inequality. Our approximate solution can be computed efficiently thanks to the two relaxations presented: Step 1 (non-conforming approximation) and Step 2 (bound conditioner). We expect that the loss of sharpness due to the non-conforming approximation is relatively small as long as our port reduction procedure provides an effective port expansion (as indicated in Remark 2); and we know that the loss of sharpness due to the bound conditioner is small as long as the smallest eigenvalue  $\lambda_{\min}(\mu)$  associated with (68) is of order unity and the eigenvalue lower bound  $\lambda_{\min, \text{LB}}(\mu)$  is relatively sharp.

## 5 Computational Considerations

### 5.1 Procedures

We first discuss the computation of the port-reduced solution  $\mathbb{U}_A(\mu)$  of the system (26). To this end we write for instantiated component  $i$  the (non-port-reduced) component stiffness matrix and component load vector as

$$\mathbb{A}^i(\mu_i) = \begin{bmatrix} \mathbb{A}_{AA}^i(\mu_i) & \mathbb{A}_{AI}^i(\mu_i) \\ \mathbb{A}_{IA}^i(\mu_i) & \mathbb{A}_{II}^i(\mu_i) \end{bmatrix}, \quad \mathbb{F}^i(\mu_i) = \begin{bmatrix} \mathbb{F}_A^i(\mu_i) \\ \mathbb{F}_I^i(\mu_i) \end{bmatrix}, \quad (97)$$

respectively, where again the matrix and vector blocks refer to couplings between degrees of freedom marked as active and degrees of freedom marked as inactive, but now on a *component*-matrix level. To form (26) we only need to form for each instantiated component  $i$  the active component matrix  $\mathbb{A}_{AA}^i(\mu_i)$  and component vector  $\mathbb{F}_A^i(\mu_i)$ ; assembly of (26) then follows a direct stiffness procedure analogous to Algorithm 1. For instantiated component  $i$ , let  $n_A^i = \sum_{j=1}^{n_{\mathcal{M}(i)}} n_{A,i,j}^\gamma$  and  $n_I^i = \sum_{j=1}^{n_{\mathcal{M}(i)}} n_{I,i,j}^\gamma$  be the total number of active and inactive degrees of freedom, respectively; thus  $\mathbb{A}_{AA}^i(\mu_i) \in \mathbb{R}^{n_A^i \times n_A^i}$ ,  $\mathbb{A}_{IA}^i(\mu_i) \in \mathbb{R}^{n_A^i \times n_I^i}$ , and  $\mathbb{A}_{II}^i(\mu_i) \in \mathbb{R}^{n_I^i \times n_I^i}$ .

We next discuss the computation of the error bound in Proposition 2. There are two key ingredients: the non-conforming “(B’)-solves” in (79) and (91), and the calculation of the residuals  $\mathbb{R}'(\mu)$  and  $\mathbb{R}'_{\text{eig}}(\mu)$ . We first consider the former, and then the latter.

Both our eigenvalue bound in Proposition 1 and our error bound in Proposition 2 necessitate a global solve of the form  $z(\mu) = (\mathbb{B}')^{-1}\mathbb{R}'(\mu)$ . However thanks to the  $n_I^i$  duplicated degrees of freedom we shall in actual practice never require explicit formation or inversion of  $\mathbb{B}'$ . This significant computational saving is effected through elimination of the uncoupled degrees of freedom on a component-matrix level: the global system for  $z(\mu)$  is only of size  $n_A$ . We illustrate this point by consideration of a system consisting of only two components with instantiated component stiffness matrices  $\mathbb{A}^1(\mu)$  and  $\mathbb{A}^2(\mu)$  (for which we invoke the particular interpretation in (97)). The Schur complement system matrix  $\mathbb{A}(\mu)$  for this system (obtained through Algorithm 1) is then

$$\mathbb{A}(\mu) = \begin{bmatrix} \mathbb{A}_{AA}^1(\mu_1) + \mathbb{A}_{AA}^2(\mu_2) & \mathbb{A}_{AI}^1(\mu_1) + \mathbb{A}_{AI}^2(\mu_2) \\ \mathbb{A}_{IA}^1(\mu_1) + \mathbb{A}_{IA}^2(\mu_2) & \mathbb{A}_{II}^1(\mu_1) + \mathbb{A}_{II}^2(\mu_2) \end{bmatrix}; \quad (98)$$

the corresponding *expanded* system matrix  $\mathbb{A}'(\mu)$  is<sup>7</sup>

$$\mathbb{A}'(\mu) = \begin{bmatrix} \mathbb{A}_{AA}^1(\mu_1) + \mathbb{A}_{AA}^2(\mu_2) & \mathbb{A}_{AI}^1(\mu_1) & \mathbb{A}_{AI}^2(\mu_2) \\ \mathbb{A}_{IA}^1(\mu_1) & \mathbb{A}_{II}^1(\mu_1) & \mathbf{0} \\ \mathbb{A}_{IA}^2(\mu_2) & \mathbf{0} & \mathbb{A}_{II}^2(\mu_2) \end{bmatrix}. \quad (99)$$

Recall that the difference between (98) and (99) is that the latter does not reflect couplings between degrees of freedom that are marked as inactive (on the shared global port).

We thus write  $\mathbb{B}'z = \mathbb{R}'(\mu)$  as

$$\begin{bmatrix} \mathbb{B}_{AA}^1 + \mathbb{B}_{AA}^2 & \mathbb{B}_{AI}^1 & \mathbb{B}_{AI}^2 \\ \mathbb{B}_{IA}^1 & \mathbb{B}_{II}^1 & \mathbf{0} \\ \mathbb{B}_{IA}^2 & \mathbf{0} & \mathbb{B}_{II}^2 \end{bmatrix} \begin{bmatrix} z_A(\mu) \\ z_I^1(\mu) \\ z_I^2(\mu) \end{bmatrix} = \begin{bmatrix} \mathbb{R}_A(\mu) \\ \mathbb{R}_I^1(\mu) \\ \mathbb{R}_I^2(\mu) \end{bmatrix}. \quad (100)$$

Next, from (100) we note that

$$[\mathbb{B}_{AA}^1 + \mathbb{B}_{AA}^2 - \mathbb{B}_{AI}^1(\mathbb{B}_{II}^1)^{-1}\mathbb{B}_{IA}^1 - \mathbb{B}_{AI}^2(\mathbb{B}_{II}^2)^{-1}\mathbb{B}_{IA}^2]z_A(\mu) = \mathbb{R}_A(\mu) - \mathbb{B}_{AI}^1(\mathbb{B}_{II}^1)^{-1}\mathbb{R}_I^1(\mu) - \mathbb{B}_{AI}^2(\mathbb{B}_{II}^2)^{-1}\mathbb{R}_I^2(\mu). \quad (101)$$

We may thus obtain  $z(\mu)$  by consideration of a second Schur complement: we first solve local problems of size  $n_I^1$  and  $n_I^2$  on component 1 and 2, respectively, and then a global problem of size  $n_A$  for  $z_A(\mu)$ ; we finally recover  $z(\mu)$  by standard back-substitution as  $z_I^i = (\mathbb{B}_{II}^i)^{-1}(\mathbb{R}_I^i - \mathbb{B}_{IA}^i z_A)$ . The extension of this procedure to a system with an arbitrary number of components and ports is straightforward.

We now state

**Conjecture 2.** *Assume that  $n_{A,i,j}^\gamma \geq 1$  (recall that  $n_{A,i,j}^\gamma$  is the number of active modes on port  $\gamma_{i,j}$  of component  $i$ ). Then for  $1 \leq i \leq I$  the symmetric matrix  $\mathbb{B}_{II}^i$  is positive definite.*

---

<sup>7</sup>Thus here,  $D = \begin{bmatrix} \mathbb{I}_A & \mathbf{0} \\ \mathbf{0} & \mathbb{I}_I \\ \mathbf{0} & \mathbb{I}_I \end{bmatrix}$  for identity matrix blocks  $\mathbb{I}_*$  of appropriate dimension  $n_A$  or  $n_I$ .

*Sketch of proof.* We consider the Laplace equation in a component with domain  $\Omega_1$  and a single local port  $\gamma_{1,1}$ ; we associate to this port  $n_{A,1,1}^\gamma \geq 1$  active degrees of freedom (thus here  $n_A^1 = n_{A,1,1}^\gamma$  and  $n_I^1 = n_{I,1,1}^\gamma$ ). We consider homogeneous Neumann boundary conditions on all non-port boundaries of  $\Omega_1$ . To  $v \in \mathbb{R}^{n_I^1}$  we associate a function  $w = \sum_{k=1}^{n_I^1} v_k \phi_{1,1,k+n_{A,1,1}^\gamma}$ . In this case we obtain

$$v^T \mathbb{B}_I^1 v = a_1(w, w) = |w|_{H^1(\Omega_1)}^2 \geq 0. \quad (102)$$

Thus if  $v^T \mathbb{B}_I^1 v = 0$  we must have  $w = c$  for a constant  $c$ . But as the inactive port modes each has zero mean, we must have  $w = c = 0$ , and thus due to linear independence of the port modes we conclude that  $v_k = 0$ ,  $1 \leq k \leq n_I^1$ , since the  $\phi_{1,1,k+n_{A,1,1}^\gamma}$  are non-zero.  $\square$

Next we consider the calculation of the residual  $\mathbb{R}'(\mu) = \mathbb{F}'(\mu) - \mathbb{A}'(\mu) \hat{\mathbb{U}}_A'(\mu)$ . By inspection we note for our two-component system that

$$\begin{aligned} \mathbb{R}'(\mu) &= \begin{bmatrix} \mathbb{R}_A(\mu) \\ \mathbb{R}_I^1(\mu) \\ \mathbb{R}_I^2(\mu) \end{bmatrix} = \begin{bmatrix} \mathbb{F}_A(\mu) \\ \mathbb{F}_I^1(\mu_1) \\ \mathbb{F}_I^2(\mu_2) \end{bmatrix} - \begin{bmatrix} \mathbb{A}_{AA}(\mu) & \mathbb{A}_{AI}^1(\mu_1) & \mathbb{A}_{AI}^2(\mu_2) \\ \mathbb{A}_{IA}^1(\mu_1) & \mathbb{A}_{II}^1(\mu_1) & \mathbf{0} \\ \mathbb{A}_{IA}^2(\mu_2) & \mathbf{0} & \mathbb{A}_{II}^2(\mu_2) \end{bmatrix} \begin{bmatrix} \mathbb{U}_A(\mu) \\ \mathbf{0} \\ \mathbf{0} \end{bmatrix} \\ &= \begin{bmatrix} \mathbb{F}_A(\mu) - \mathbb{A}_{AA}(\mu) \mathbb{U}_A(\mu) \\ \mathbb{F}_I^1(\mu_1) - \mathbb{A}_{IA}^1(\mu_1) \mathbb{U}_A(\mu) \\ \mathbb{F}_I^2(\mu_2) - \mathbb{A}_{IA}^2(\mu_2) \mathbb{U}_A(\mu) \end{bmatrix} = \begin{bmatrix} \mathbf{0} \\ \mathbb{F}_I^1(\mu_1) - \mathbb{A}_{IA}^1(\mu_1) \mathbb{U}_A^1(\mu) \\ \mathbb{F}_I^2(\mu_2) - \mathbb{A}_{IA}^2(\mu_2) \mathbb{U}_A^2(\mu) \end{bmatrix}. \quad (103) \end{aligned}$$

Note that the first  $n_A$  entries in the residual vector are zero, and that in general we may obtain the local residuals  $\mathbb{R}_I^i(\mu)$  by component-local evaluation

$$\mathbb{R}_I^i(\mu) = \mathbb{F}_I^i(\mu_i) - \mathbb{A}_{IA}^i(\mu_i) \hat{\mathbb{U}}_A^i(\mu), \quad (104)$$

where  $\hat{\mathbb{U}}_A^i(\mu)$  is extracted from  $\hat{\mathbb{U}}_A(\mu)$  for the degrees of freedom associated with component  $i$ . An analogous procedure holds for the computation of the eigenproblem residual  $\mathbb{R}_{\text{eig}}(\mu)$ .

## 5.2 Computational Costs and Savings

We first comment briefly on the computational cost associated with the port-reduced solution  $\mathbb{U}_A(\mu)$ : as the active system (26) is only of size  $n_A$  the online cost associated with formation of  $\mathbb{A}_{AA}(\mu)$  scales as  $n_A$ , and the online cost associated with solution of (26) scales as  $(n_A)^\ell$ , where  $\ell > 1$  depends on the sparsity pattern of  $\mathbb{A}_{AA}(\mu)$  and the sparse solver invoked. Our goal is  $n_A \ll n_{\text{SC}}$ , which, if realized, will dramatically reduce the online data footprint and online computational cost relative to the non-port-reduced alternative.

We next comment on the computational cost associated with the *a posteriori* error bound of Proposition 2. There are three sources to the computational efficacy of the error bound procedure: the non-conforming nature of the error bound approximation; the parameter-independent bound conditioner; and efficient residual calculation.

First, the non-conforming approach requires only relatively small (size  $n_A$ ) and sparse system-level solves (101); most of the computational work is performed on the component-matrix level in the local  $\mathbb{B}_I^i$ -solves.

Second, as the  $\mathbb{B}_i$  are independent of  $\mu_i$  we may pre-compute and store these matrices in the component library. To wit, we associate with each *archetype* component  $m$  a reference component matrix  $\hat{\mathbb{B}}^m$ . For each instantiated component  $i$ ,  $1 \leq i \leq I$ , we may then for given  $n_{A,p}^\Gamma$  (on all global ports  $\Gamma_p$  associated with component  $i$ ) and  $\mathbb{R}_I^i(\mu)$  select the reference matrix  $\mathbb{B}^i = \hat{\mathbb{B}}^{\mathcal{M}(i)}$  from the library and form the Schur complement system (101). We emphasize that the non-conforming system preconditioner matrix  $\mathbb{B}'$  is never explicitly formed.

Third, as demonstrated in (103), the residual  $\mathbb{R}'(\mu)$  can be assembled locally on the component-matrix level, and does *not* require formation of the parameter-dependent matrices  $\mathbb{A}_{II}^i(\mu)$ . This latter fact is crucial in the context of the SCRBE — our computational vehicle for these port reduction procedures — for which

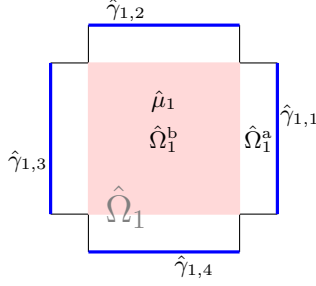


Figure 2: An archetype component with four local ports and one parameter.

it is the storage and cost associated with *formation* of the  $\mathbb{A}_{\text{II}}^i(\mu)$  matrices that pose an online computational challenge (in particular when  $n_A \ll n_I$ ). The matrices  $\mathbb{B}_{\text{II}}^i$  do not represent a computational issue as the formation of these matrices can be performed offline.

Recall that on component  $i$ ,  $n_A^i$  and  $n_I^i$  denote the number of total active and inactive degrees of freedom, respectively. We may then summarize the computational cost associated with a *posteriori* error bound calculation for our system instantiated from a library of  $M$  archetypes as follows. First, the cost associated with formation of (101) scales as  $M \max_{1 \leq i \leq I} ((n_I^i)^3 + n_A^i (n_I^i)^2) + I \max_{1 \leq i \leq I} (n_A^i)^2$  (we use Cholesky factorization for the component-local  $\mathbb{B}_{\text{II}}^i$ -solves, and perform these solves only once for each archetype component); second, the cost associated with the solve (101) scales as  $(n_A)^\ell + I \max_{1 \leq i \leq I} (n_I^i)^2$  including back-substitution; and third, the cost associated with residual calculation scales as  $I \max_{1 \leq i \leq I} (n_A^i n_I^i)$ . We emphasize that in contrast to earlier approaches [20] our *a posteriori* error bound computation does not invoke the underlying (component-interior) FE discretization.

Additional computational economies may be realized if we consider the number of active modes  $n_{A,i,j}^\gamma$  on port  $\gamma_{i,j}$  as fixed for all instantiations of ports within the same port group. In this case we may pre-extract the  $\hat{\mathbb{B}}_{\text{II}}^m$ ,  $\hat{\mathbb{B}}_{\text{IA}}^m$ , and  $\hat{\mathbb{B}}_{\text{AI}}^m$  from  $\hat{\mathbb{B}}^m$ , and perform an offline Cholesky factorization of the  $\hat{\mathbb{B}}_{\text{II}}^m$ ; we thus reduce the online cost of formation of (101) to  $M \max_{1 \leq i \leq I} n_A^i (n_I^i)^2 + I \max_{1 \leq i \leq I} (n_A^i)^2$ . In fact, we may even precompute and associate to an archetype component the terms  $\hat{\mathbb{B}}_{\text{AI}}^m (\hat{\mathbb{B}}_{\text{II}}^m)^{-1} \hat{\mathbb{B}}_{\text{IA}}^m$  that make up the Schur complement in (101), in which case formation of (101) is reduced to  $I \max_{1 \leq i \leq I} (n_A^i)^2$ . Even further computational savings may be realized for a *fixed system topology* subject to repeated solution for different parameter values, in which case we may pre-compute and pre-factorize the left hand side of (101).

## 6 Numerical Results

In this section we present numerical results which illustrate the port approximation and reduction procedure and which furthermore demonstrate the *a posteriori* error bounds with respect to rigor and sharpness. Our goal here is to present the port approximation and error bound framework, and hence we consider a simple two-dimensional Laplace model problem. Substantial computational savings are realized only for larger (e.g. 3D thermal or linear elasticity) problems which we shall consider in a future publication.

We consider the single archetype component illustrated in Figure 2. For this component we shall always consider the same port space for all ports; however we shall consider both empirical modes and pure Legendre modes as basis functions for the port space, and hence in fact we consider two different (one-component) libraries.

The archetype component parameter  $\hat{\mu}_1$  is the “thermal conductivity” in the shaded region of the component,  $\hat{\Omega}_1^b$ , relative to the conductivity in the unshaded region,  $\hat{\Omega}_1^a$ ; we consider  $\hat{\mu}_1 \in \hat{\mathcal{D}}^1 = [0.1, 10]$ . The archetype component has four local ports; on the top port we have the option of enforcing a unity inward flux through a Boolean “parameter”  $B \in \{0, 1\}$ ; on any of the ports we can elect to impose Dirichlet conditions (on the assembled system). On the non-port parts of the boundary we consider homogeneous Neumann

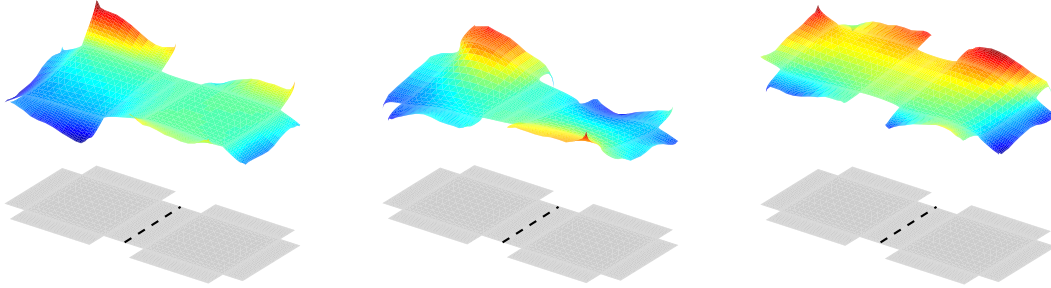


Figure 3: The three first solutions for the two-component pairwise training procedure of Algorithm 2. The system geometry is shown in gray and the shared port is indicated with a dashed line; note random boundary conditions are assigned on the six non-shared ports.

boundary conditions. The archetype bilinear and linear forms are then given as

$$\hat{a}_1(w, v; \hat{\mu}_1) = \int_{\hat{\Omega}_1^a} \nabla w \cdot \nabla v + \hat{\mu}_1 \int_{\hat{\Omega}_1^b} \nabla w \cdot \nabla v, \quad (105)$$

and

$$\hat{f}_1(v; \hat{\mu}_1) = B \int_{\hat{\gamma}_{1,2}} v, \quad (106)$$

respectively, for  $w, v \in H^1(\hat{\Omega}_1)$ .

For the underlying FE discretization we employ here standard spectral elements [22]; the component domain  $\hat{\Omega}_1$  admits a natural decomposition into five rectangular elements, each of which is discretized with an approximation space of polynomial order 15 in each spatial direction. This discretization yields a discrete space  $X_1^h(\hat{\Omega}_1)$  of dimension 1216 and port spaces  $P_{1,j}^h$  of dimension  $\mathcal{N}_{1,j}^\gamma = 16$ ,  $1 \leq j \leq 4$ .

For the bubble functions associated with the static condensation we shall consider the SCRBE method as discussed in Section 2.3. As the focus in this paper is not the error (and bound) due to RB approximation but rather the error (and bound) due to port reduction, each of the RB approximation spaces are constructed such that the error associated with each RB bubble function is relatively small — smaller than  $10^{-5}$  over  $\hat{\mathcal{D}}^1$ .<sup>8</sup> However, for our compliance output error bound results below, we do nevertheless incorporate in our port reduction output error bounds (Corollary 1) the additional contribution of the RB error bounds as developed in Appendix A.

**Empirical Port Modes.** First, we consider pairwise training — Algorithm 2 — for the construction of the empirical port modes used in our numerical results. In the case of our particular archetype component we note that we may consider a single port group (of interconnectable local ports), and moreover, due to the spatial symmetry of the component, we may consider only one pair of instantiated archetypes for the generation of empirical modes.

We thus execute Algorithm 2 once for a single pair of components for  $N_{\text{samples}} = 200$  and  $\eta = 2$  to obtain the set  $S_{\text{group}}$  of cardinality 200 (note here  $S_{\text{pair}} = S_{\text{group}}$ ). In Figure 3 we show solution fields for this component pair for the first three iterations of the algorithm; note that random but still somewhat smooth (thanks to  $\eta = 2$ ) boundary conditions are imposed on the six non-connected ports.

In Figure 4 (left) we show the solution at the interior global port associated with each of the three (two-component) system solutions of Figure 3; we note the very smooth behavior compared to the assigned

<sup>8</sup>This number is calculated (in the offline stage) over a parameter training set  $\Xi \subset \hat{\mathcal{D}}^1$  of finite cardinality; hence for parameters outside the training set, efficiently (online) computable *a posteriori* RB error bounds [25] are crucial to determine the accuracy of the RB approximations.



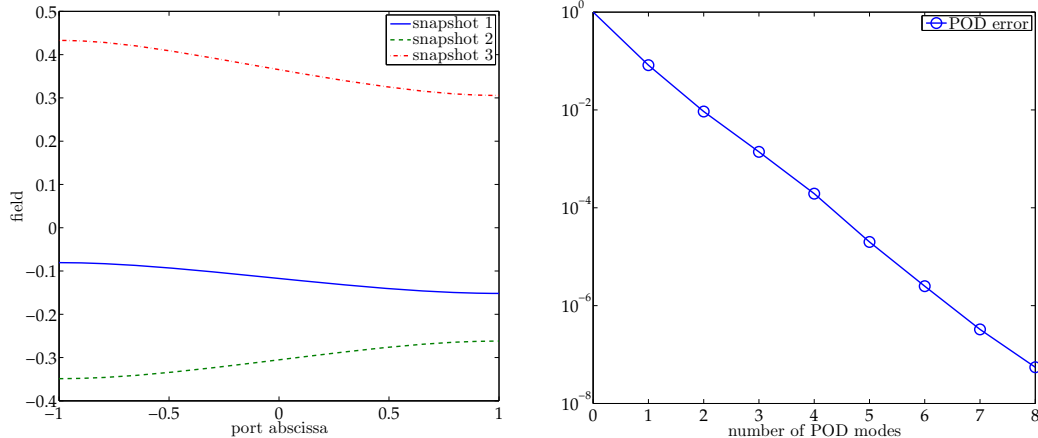


Figure 4: Left: the first three extracted port snapshots from Algorithm 2 (prior to subtraction of constant). Right: the POD errors associated with the first eight POD modes of the snapshot set obtained with Algorithm 2; recall that we subtract the mean from each snapshot prior to POD.

boundary conditions. This is not surprising as we expect that for our elliptic problem the solution associated with a high wavenumber port boundary condition will decay exponentially fast away from the port and into the component.<sup>9</sup> This observation is promising for port reduction: we expect that for any instantiated system the solution at any interior port is very smooth and admits a good approximate modal representation (33) with only a few terms.

We perform the POD of the function set  $S_{\text{group}}$  and retain the 8 first POD modes to obtain the spaces  $Y_{1,j}$  of dimension  $y_{1,j} = 9$ ,  $1 \leq j \leq 4$ ; recall that in addition to the POD modes we include in the basis for  $Y_{1,j}$  the constant mode as the first basis function  $\chi_{1,j,1}$ . In Figure 4 (right) we show the POD error (over the  $N_{\text{samples}} = 200$  snapshots) associated with the 8 POD modes (with constant subtracted from snapshots prior to POD).<sup>10</sup> For our numerical results below we shall invoke this empirical port space with  $y_{1,j} = 9$ ,  $1 \leq j \leq 4$ , empirical modes (including the constant); note that we may still consider any  $n_{A,p}^{\Gamma} \geq 1$ ,  $1 \leq p \leq n^{\Gamma}$ . The empirical modes are complemented with 7 orthogonal-complement “Legendre” modes (36) to complete the discrete space. As an alternative discrete space, we shall also consider a pure Legendre port space consisting of 16 Legendre modes, corresponding to  $y_{1,j} = 0$ ,  $1 \leq j \leq 4$ . For all computations below the reference bound conditioner component matrix is  $\hat{\mathbb{B}}^1 = \mathbb{A}^1(\hat{\mu}_1 = 1)$  (and hence the reference system parameter  $\mu_{\text{ref}}$  for an  $I$ -component system is the  $I$ -tuple of ones).

When, on each global port  $p$ , we consider all  $\mathcal{N}_p^{\Gamma} = 16$  port modes, either empirical, plus “Legendre” complement or pure Legendre, we of course reduce the error due to port reduction to zero; hence for this particular problem, we only realize computational savings if we can retain  $n_{A,p}^{\Gamma} \ll 16$  port modes for the approximation. (In general, we also wish and indeed observe that the number of *empirical* modes required (for fixed accuracy) is independent of  $\mathcal{N}_{m,j}^{\gamma}$  as  $\mathcal{N}_{m,j}^{\gamma} \rightarrow \infty$ .) For 2D problems (1D ports), there is relatively little opportunity for computational savings, and hence we do not provide timings in the current paper. However, for 3D problems (2D ports) and in particular for vector-valued fields (such as linear elasticity) we often have  $\mathcal{N}_{m,j}^{\gamma} \sim \mathcal{O}(10^3)$  even for rather modest FE discretizations, in which case there is much opportunity for meaningful port reduction.

<sup>9</sup>Indeed, this may readily be seen for a simple case: consider of a rectangular component domain  $\Omega = [0, 1] \times [0, 1]$  with a single port on the entire side  $y = 0$ . Apply to this side a “Fourier” port boundary condition  $u(x, 0) = \cos(k\pi x)$ , apply zero Dirichlet conditions on the side  $y = 1$ , and apply homogeneous Neumann boundary conditions on the sides  $x = 0$  and  $x = 1$ . In this case the analytical solution to the Laplace equation over the domain  $\Omega$  is found via separation of variables as  $u(x, y) = (\cos(k\pi x)) \sinh(k\pi(1 - y)) / \sinh(k\pi)$ .

<sup>10</sup>The POD error for  $n$  POD modes is equal to the average  $L^2(\Gamma_{p^*})$  projection error (onto the  $n$ -dimensional POD space) over the  $N_{\text{samples}}$  snapshots and may be computed as the (normalized) square root of the sum of the remaining  $N_{\text{samples}} - n$  eigenvalues associated with the POD eigenproblem.

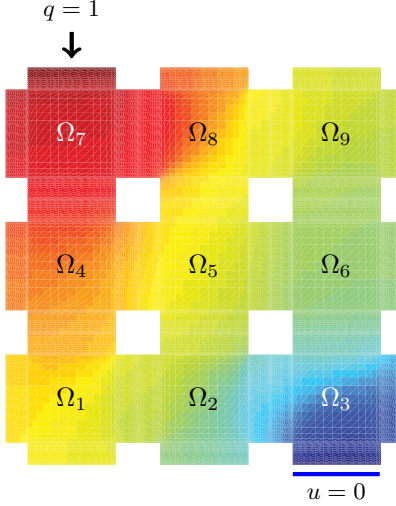


Figure 5: Example 1. System with  $I = 9$  component instantiations and  $n^\Gamma = 23$  global ports. Unity heat flux (Neumann) on top left port;  $u = 0$  Dirichlet condition on bottom right port; homogeneous Neumann conditions on other ports and boundaries. Solution plotted for particular system parameter  $\mu = (0.1, 0.2, 0.4, 0.8, 1.6, 3.2, 6.4, 0.1, 0.2)$ .

**Example 1.** As a first system, we consider the  $3 \times 3$  layout of component instantiations illustrated in Figure 5; the system thus has  $I = 9$  components and nine independent parameters. As indicated, we impose a homogeneous Dirichlet condition on the bottom right port, a unity inward “heat” flux  $q = 1$  on the top left port, and homogeneous Neumann boundary conditions on all other boundary ports. The system thus has  $n^\Gamma = 23$  global ports in total, of which 12 are in the interior and serve to connect two neighboring components. The size of the associated non-port-reduced static condensation system (22) is  $n_{SC} = \mathcal{N}_p^\Gamma n^\Gamma = 368$ . The compliance output for this system is the integrated “temperature”  $s(\mu) = \int_{\gamma_{7,2}} u(\mu)$  on the heated (top left) port. Below we shall consider the relative compliance output error and relative *a posteriori* output error bound due to port reduction as well as SCRBE bubble function approximation.

We first consider a particular value  $\mu = (0.1, 0.2, 0.4, 0.8, 1.6, 3.2, 6.4, 0.1, 0.2)$  for the system parameter, and we consider the  $y_{1,j} = 9$  empirical port space as constructed in the previous subsection for the port approximation. In Figure 6 (left) we show the relative output error (blue),  $(s^h(\mu) - \tilde{s}_A(\mu))/\tilde{s}_A(\mu)$ , and relative output error bound (red)  $(\Delta^u(\mu))^2/\tilde{s}_A(\mu)$  (modified to account for non-zero RB errors as discussed in Appendix A), as functions of the number of active modes on each global port (the same number on all ports),  $n_{A,p}^\Gamma$ : we observe very rapid convergence, and equally importantly the error *bound* also converges exponentially fast — the output error bound effectivity<sup>11</sup> is  $\mathcal{O}(100)$ . After eight modes there is not much room for further error decay due to RB bubble function approximation. The size of the port-reduced static condensation system (26) is  $n_A = n^\Gamma n_{A,p}^\Gamma = 23n_{A,p}^\Gamma$  (recall we choose the same number of active port modes for all ports).

Next, in Figure 6 (right) we show the error in the eigenvalue approximation,  $\lambda_{\min}(\mu) - \lambda_{\min, LB}(\mu)$ . Note that for this example, we confirm *a posteriori* that the eigenvalue proximity assumption (80) is satisfied for  $n_{A,p}^\Gamma \geq 2$ . We provide further comment on this result below.

We also consider the alternative Legendre eigenmode ( $y_{1,j} = 0$ ) port space. The output errors (green) and output error bounds (light blue) as functions of the number of active port modes on each port are shown in Figure 7 (superposed on the results of Figure 6). We note that the Legendre modes also exhibit rapid convergence thanks to the relatively smooth solutions at the ports, although the convergence is not as rapid as for the empirical modes. Indeed, in this case it is likely that the empirical modes will be quite

<sup>11</sup>We define the effectivity to be the error bound divided by the true error.

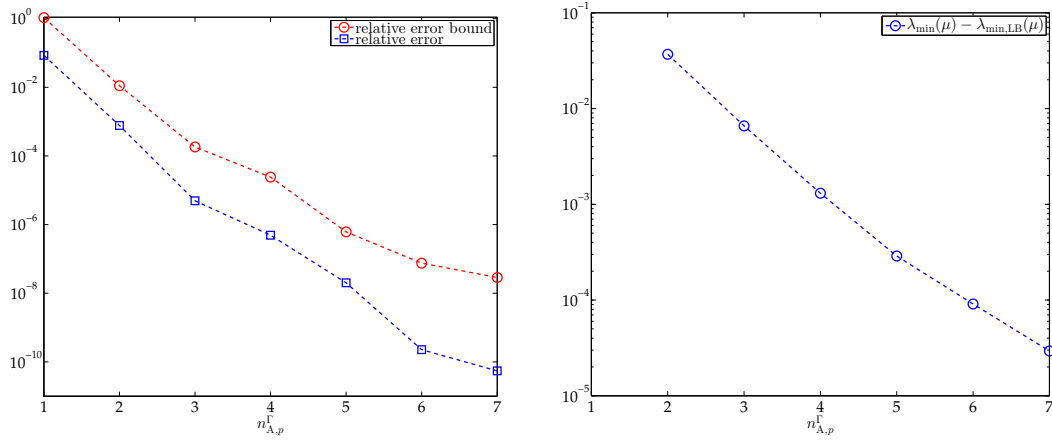


Figure 6: Example 1. Left: Relative output error and relative output error bound based on the empirical ( $y_{1,j} = 9$ ) port space as functions of  $n_{A,p}^\Gamma$ , the number of empirical port modes. Right: Eigenvalue approximation error.

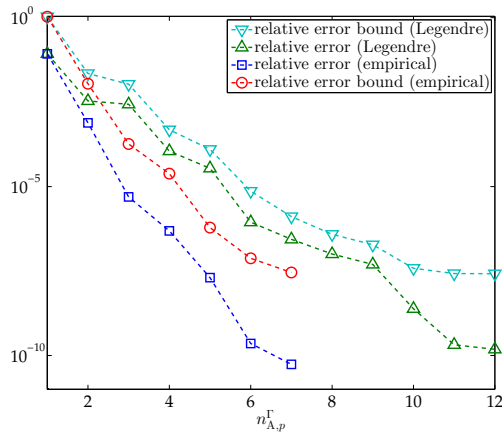


Figure 7: Example 1. Relative output error and relative output error bound for empirical ( $y_{i,j} = 9$ ) and Legendre ( $y_{i,j} = 0$ ) port modes.

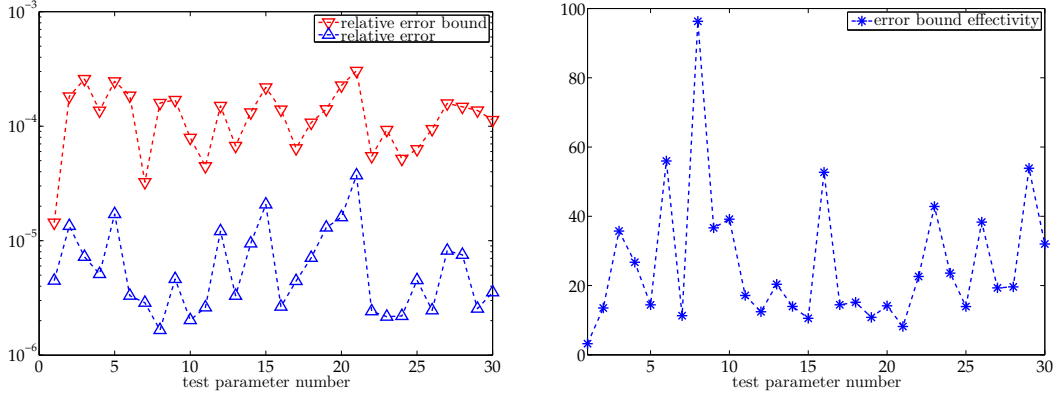


Figure 8: Example 1. Left: Relative output errors and relative output error bounds over a parameter test set  $\Xi_{\text{test}}$  for the case  $n_{A,p}^\Gamma = 3$ . Right: Output error bound effectivities.

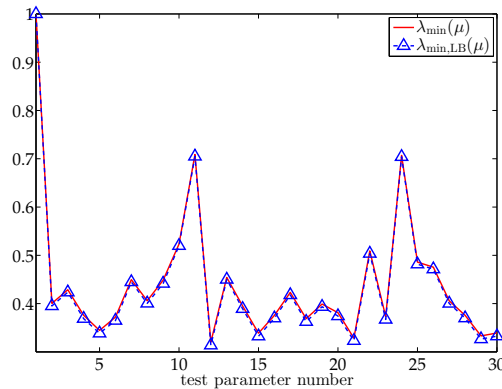


Figure 9: Example 1. Eigenvalues  $\lambda_{\min}(\mu)$  (red) and bounds  $\lambda_{\min, \text{LB}}(\mu)$  (blue) over a parameter test set  $\Xi_{\text{test}}$  for the case  $n_{A,p}^\Gamma = 3$ .

similar to the Legendre modes. This is in some sense confirmation that the empirical modes are “good,” but also an indication that empirical modes are not overly needed in this two-dimensional case. However, for three-dimensional problems (with two-dimensional ports) we expect that the pure (even singular) eigenmode convergence will deteriorate and that empirical modes will be crucial.

Finally, we again consider the empirical modes and fix  $n_{A,p}^\Gamma = 3$ ,  $1 \leq p \leq 23$ . We consider a test set  $\Xi_{\text{test}} \subset \mathcal{D}$  of 30 system parameter values: the first parameter value is  $\mu = \mu_{\text{ref}} = (1, 1, 1, 1, 1, 1, 1, 1)$ ; the remaining 29 parameter values are random. For each parameter value we compute the relative output error and relative output error bound as shown in Figure 8 (left); in Figure 8 (right) we show the associated bound effectivities. We note that the bounds are very sharp — we typically obtain  $\mathcal{O}(10)$  effectivities.

Note that for all cases considered here we obtain a rather small output error bound with a modest number of active port modes, and furthermore the output error bounds are rather sharp. The former is a reflection of the good approximation properties of the empirical port modes. The latter is a reflection of the good non-conforming error approximation, but also of an effective bound conditioner, which is implicated by the relatively large (order unity) smallest eigenvalues and sharp eigenvalue lower bounds: in Figure 9 we show the eigenvalues  $\lambda_{\min}(\mu)$  (red) and the eigenvalue lower bounds  $\lambda_{\min, \text{LB}}(\mu)$  (blue) over the test parameter set  $\Xi_{\text{test}}$ . In this case the eigenvalue proximity assumption (80) holds for each of the test parameters. We can also flush out the role of the non-conforming approximation. In particular, the first test parameter is special as in this case  $\mathbb{E}'(\mu) = \mathbb{E}'_{\mathbb{B}}(\mu)$  since  $\mathbb{B}' = \mathbb{A}'(\mu_{\text{ref}} = \mu)$  (the bound conditioner is perfect); we further note

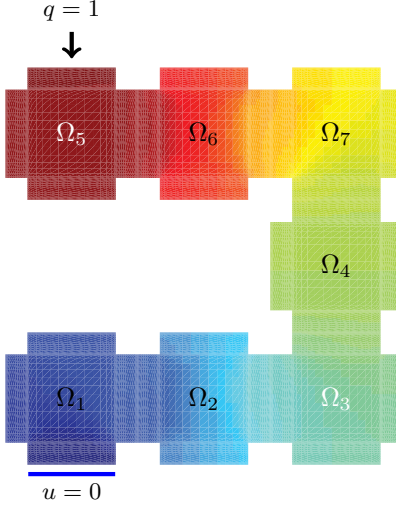


Figure 10: Example 2. System with  $I = 7$  component instantiations and  $n^\Gamma = 21$  global ports. Unity heat flux (Neumann) on top left port;  $u = 0$  Dirichlet condition on bottom left port; homogeneous Neumann conditions on other ports and boundaries. Solution plotted for particular system parameter  $\mu = (0.1, 0.2, 0.4, 3.2, 6.4, 0.1, 0.2)$ .

from (76) and (78) that  $\lambda_{\min}(\mu_{\text{ref}}) = \lambda_{\min, \text{LB}}(\mu_{\text{ref}}) = 1$ . Hence for this first test parameter our output error bound is in fact the bound of Lemma 1. We observe that the associated bound effectivity is rather close to unity (more precisely 3.218) and hence the non-conforming approximation is clearly very accurate.

**Example 2.** As our second system, we consider the “horseshoe” layout of component instantiations illustrated in Figure 10; the system has  $I = 7$  components and seven independent parameters. As indicated, we impose a homogeneous Dirichlet condition on the bottom left port, a unity inward “heat” flux  $q = 1$  on the top left port, and homogeneous Neumann boundary conditions on all other boundary ports. The system thus has  $n^\Gamma = 21$  global ports in total, of which 6 are in the interior and hence connect two neighboring components. The size of the associated non-port-reduced static condensation system (22) is  $n_{\text{SC}} = 336$ . The compliance output for this system is the integrated “temperature”  $s(\mu) = \int_{\gamma_{5,2}} u$  on the heated (top left) port.

We again first consider a particular value  $\mu = (0.1, 0.2, 0.4, 3.2, 6.4, 0.1, 0.2)$  for the system parameter. In Figure 11 (left) we show for this parameter value the relative output error and relative output error bounds as a function of the number of port modes for both the empirical port space ( $y_{1,j} = 9$ ) and the pure Legendre port space ( $y_{1,j} = 0$ ). The results are comparable to the results for Example 1 in terms of both error decay and error bound sharpness. Next, in Figure 11 (right) we show the eigenvalue approximation error  $\lambda_{\min}(\mu) - \lambda_{\min, \text{LB}}(\mu)$  for the empirical port space; we confirm that the eigenvalue proximity assumption (80) holds for  $n_{\text{A},p}^\Gamma \geq 2$ .

Example 1 and Example 2 collectively also highlight another key aspect of both the SCRBE framework in [15] and of the port approximation framework introduced here: the SCRBE and associated port approximation data is constructed “offline” and is associated with the archetype library components. “Online,” we may then rapidly compute port-reduced SCRBE approximations *and* associated *a posteriori* error bounds for *any* topological configuration of the library components and for *any* assigned system parameter values.

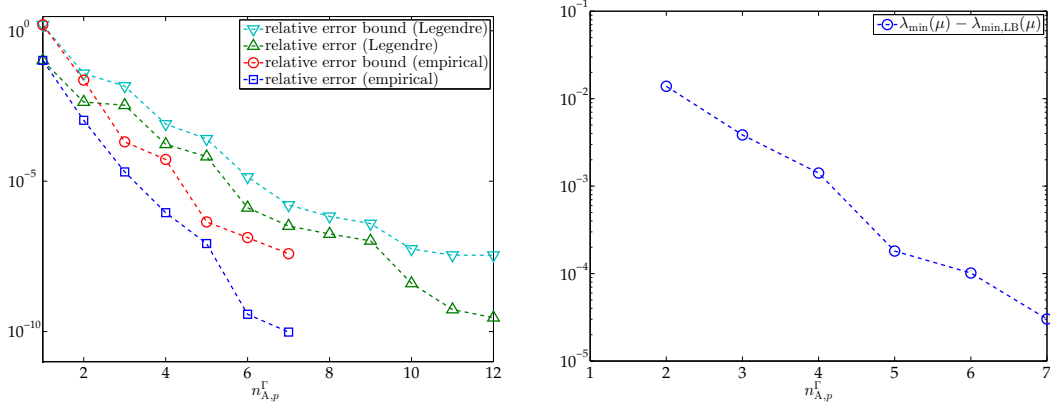


Figure 11: Example 2. Left: Relative output error and relative error bounds as functions of  $n_{A,p}^\Gamma$  for the empirical ( $y_{1,j} = 9$ ) and for the Legendre ( $y_{1,j} = 0$ ) port modes. Right: Eigenvalue approximation error for the empirical port modes.

## 7 Concluding Remarks

We have introduced a general port-reduction approximation and a *a posteriori* error estimation framework for component-based static condensation. Empirical modes tailored to component connectivity and parameter dependence through pairwise training provide rapidly convergent expansions for the solution associated with the ports; truncation of these expansions lead in turn to a Schur complement system of reduced size. Our numerical results for a Laplace model problem demonstrate good approximation properties for these truncated empirical port expansions.

The error in the port-reduced static condensation is rigorously bounded *a posteriori* under a plausible but in practice not verified eigenvalue proximity assumption. As we obtain an *a posteriori* error bound through (approximate) solution of the error-residual equation — rather than direct residual evaluation — our error bound is rather sharp. The computational tractability of our *a posteriori* error bound is achieved through two relaxations of the error-residual equation: a non-conforming error approximation, and a bound conditioner.

The port approximation and *a posteriori* error bound framework introduced here is particularly relevant within the SCRBE [15] method for parameter-dependent component-based systems, in which reduced basis [25] approximations are considered for the component-local bubble functions. In this context there is a natural offline-online separation of the computational effort, to which the port reduction procedures presented here are well-suited.

We note that the static condensation framework is in general not applicable to non-linear partial differential equations, and thus the SCRBE method does not directly extend to this class of problems (although isolated non-linearities might be treated through a FE-SCRBE hybrid approach [1]). There are, however, many relevant applications of linear partial differential equations that we may consider; future work includes application to acoustics [14, 16] as well as three-dimensional linear elasticity for strength assessment.

## Acknowledgements

We are grateful to Prof. E. M. Rønquist, Dr. D. B. P. Huynh, Dr. D. J. Knezevic, and Dr. S. Vallaghé for many helpful comments and fruitful discussions. This work is sponsored by the Research Council of Norway and ONR Grant N00014-11-0713.

## A Contributions from Non-Zero RB Errors

In practice, we employ the SCRBE for bubble function approximation and hence the assumption in Section 4 of exact bubble functions does not hold. We here make the necessary modifications to our energy-norm error bound in Proposition 2 such that we also bound the contribution to the error induced by RB approximation. In particular, we must make two modifications: a modified functional (70) and a modified eigenvalue lower bound  $\lambda_{\min, \text{LB}}(\mu)$ . Both of these modifications are required because in the presence of RB approximation we do not have access to the exact quantities  $\mathbb{A}'(\mu)$  and  $\mathbb{F}'(\mu)$ .

Recall that with the SCRBE our active Schur complement system is an RB approximation of (26) such that the solution  $\tilde{\mathbb{U}}'_A(\mu)$  satisfies

$$\tilde{\mathbb{A}}_{AA}(\mu)\tilde{\mathbb{U}}'_A(\mu) = \tilde{\mathbb{F}}_A(\mu), \quad (107)$$

and we thus *redefine* the error vector in this appendix as

$$\mathbb{E}(\mu) \equiv \mathbb{U}(\mu) - \hat{\mathbb{U}}_A(\mu) \in \mathbb{R}^{n_{sc}}, \quad (108)$$

where as in (42) the  $\hat{\cdot}$  indicates extension by zeros to obtain the correct vector dimension. We must also redefine the (non-conforming) residual as

$$\mathbb{R}'(\mu) \equiv \mathbb{F}'(\mu) - \mathbb{A}'(\mu)\hat{\mathbb{U}}'_A(\mu); \quad (109)$$

note the error-residual relation  $\mathbb{A}'(\mu)\mathbb{E}'(\mu) = \mathbb{R}'(\mu)$  still holds.

As we do not have access to  $\mathbb{F}'(\mu)$  and  $\mathbb{A}'(\mu)$  we introduce a residual approximation based on  $\tilde{\mathbb{A}}'(\mu)$  and  $\tilde{\mathbb{F}}'(\mu)$  as

$$\tilde{\mathbb{R}}'(\mu) \equiv \tilde{\mathbb{F}}'(\mu) - \tilde{\mathbb{A}}'(\mu)\hat{\mathbb{U}}'_A(\mu) = \mathbb{R}'(\mu) + \delta\mathbb{R}'(\mu), \quad (110)$$

where

$$\delta\mathbb{R}'(\mu) \equiv \tilde{\mathbb{F}}'(\mu) - \mathbb{F}'(\mu) + (\mathbb{A}'(\mu) - \tilde{\mathbb{A}}'(\mu))\hat{\mathbb{U}}'_A(\mu); \quad (111)$$

we also introduce a vector  $\boldsymbol{\sigma}_1(\mu)$  of RB error bounds for the individual entries in  $\delta\mathbb{R}'(\mu)$  such that

$$\boldsymbol{\sigma}_{1,i}(\mu) \geq |\delta\mathbb{R}'_i(\mu)|; \quad (112)$$

the details of this RB bubble error bound may be found in [25].

With the residual approximation (110) we now modify the functional (70) as

$$\tilde{\mathcal{J}}'_B(v; \mu) = \frac{\lambda_{\min}(\mu)}{2} v^T \mathbb{B}' v - v^T \tilde{\mathbb{R}}'(\mu); \quad (113)$$

from the corresponding Euler equation, the minimizer is given as

$$\tilde{\mathbb{E}}'_B(\mu) = \frac{1}{\lambda_{\min}(\mu)} (\mathbb{B}')^{-1} \tilde{\mathbb{R}}'(\mu). \quad (114)$$

For the minimum value we obtain

$$\begin{aligned} \tilde{\mathcal{J}}'_B(\tilde{\mathbb{E}}'_B(\mu); \mu) &= -\frac{\tilde{\mathbb{R}}'(\mu)^T (\mathbb{B}')^{-1} \tilde{\mathbb{R}}'(\mu)}{2\lambda_{\min}(\mu)} \\ &= -\frac{\mathbb{R}'(\mu)^T (\mathbb{B}')^{-1} \mathbb{R}'(\mu)}{2\lambda_{\min}(\mu)} - \frac{\tilde{\mathbb{R}}'(\mu)^T (\mathbb{B}')^{-1} \delta\mathbb{R}'(\mu)}{\lambda_{\min}(\mu)} + \frac{\delta\mathbb{R}'(\mu)^T (\mathbb{B}')^{-1} \delta\mathbb{R}'(\mu)}{2\lambda_{\min}(\mu)}, \end{aligned} \quad (115)$$

which yields

$$-2\mathcal{J}'_{\mathbb{B}}(\mathbb{E}'_{\mathbb{B}}(\mu); \mu) = \frac{\tilde{\mathbb{R}}'(\mu)^{\text{T}}(\mathbb{B}')^{-1}\tilde{\mathbb{R}}'(\mu)}{\lambda_{\min}(\mu)} - 2\frac{\tilde{\mathbb{R}}'(\mu)^{\text{T}}(\mathbb{B}')^{-1}\delta\mathbb{R}'(\mu)}{\lambda_{\min}(\mu)} + \frac{\delta\mathbb{R}'(\mu)^{\text{T}}(\mathbb{B}')^{-1}\delta\mathbb{R}'(\mu)}{\lambda_{\min}(\mu)}. \quad (116)$$

Recall from Lemma 2 that  $\|\mathbb{E}(\mu)\|_{\mathbb{A}(\mu)}^2 \leq -2\mathcal{J}'_{\mathbb{B}}(\mathbb{E}'_{\mathbb{B}}(\mu); \mu)$  and thus

$$\|\mathbb{E}(\mu)\|_{\mathbb{A}(\mu)}^2 \leq \frac{\tilde{\mathbb{R}}'(\mu)^{\text{T}}(\mathbb{B}')^{-1}\tilde{\mathbb{R}}'(\mu)}{\lambda_{\min}(\mu)} - 2\frac{\tilde{\mathbb{R}}'(\mu)^{\text{T}}(\mathbb{B}')^{-1}\delta\mathbb{R}'(\mu)}{\lambda_{\min}(\mu)} + \frac{\delta\mathbb{R}'(\mu)^{\text{T}}(\mathbb{B}')^{-1}\delta\mathbb{R}'(\mu)}{\lambda_{\min}(\mu)}. \quad (117)$$

We now introduce a constant  $C > 0$  such that

$$\delta\mathbb{R}'(\mu)^{\text{T}}(\mathbb{B}')^{-1}\delta\mathbb{R}'(\mu) \leq C\|\delta\mathbb{R}'(\mu)\|_2^2, \quad (118)$$

where  $\|\cdot\|_2$  refers to the Euclidean norm. Upon application of the RB bounds (112) we obtain

$$\|\mathbb{E}(\mu)\|_{\mathbb{A}(\mu)}^2 \leq \frac{\tilde{\mathbb{R}}'(\mu)^{\text{T}}(\mathbb{B}')^{-1}\tilde{\mathbb{R}}'(\mu)}{\lambda_{\min}(\mu)} + 2\frac{\boldsymbol{\sigma}_1(\mu)^{\text{T}}|(\mathbb{B}')^{-1}\tilde{\mathbb{R}}'(\mu)|}{\lambda_{\min}(\mu)} + C\frac{\|\boldsymbol{\sigma}_1(\mu)\|_2^2}{\lambda_{\min}(\mu)}. \quad (119)$$

We next consider the modification to the eigenvalue lower bound  $\lambda_{\min, \text{LB}}(\mu) \leq \lambda_{\min}(\mu)$ .

In the presence of RB approximation our active eigenproblem (76) (for the smallest eigenvalue and associated eigenvector) becomes

$$\tilde{\mathbb{A}}_{\text{AA}}(\mu)\tilde{v}_{\text{A},1}(\mu) = \tilde{\lambda}_{\text{A},\min}(\mu)\mathbb{B}_{\text{AA}}\tilde{v}_{\text{A},1}(\mu), \quad \tilde{v}_{\text{A},1}^{\text{T}}\mathbb{B}_{\text{AA}}\tilde{v}_{\text{A},1} = 1. \quad (120)$$

We redefine the eigenproblem residual (78) accordingly to read

$$\mathbb{R}'_{\text{eig}}(\mu) = \underbrace{\tilde{\mathbb{A}}'(\mu)\hat{v}_{\text{A},1}(\mu) - \tilde{\lambda}_{\text{A},\min}(\mu)\mathbb{B}'\hat{v}_{\text{A},1}(\mu)}_{\equiv \tilde{\mathbb{R}}'_{\text{eig}}(\mu)} + \underbrace{\delta\mathbb{A}'(\mu)\hat{v}_{\text{A},1}(\mu)}_{\equiv \delta\mathbb{R}'_{\text{eig}}(\mu)} \quad (121)$$

(where as in (77) the  $\hat{\cdot}$  indicates extension by zeros to obtain the correct vector dimension). To account for RB errors in the eigenproblem residual perturbation term  $\delta\mathbb{R}'_{\text{eig}}(\mu)$  we introduce a vector  $\boldsymbol{\sigma}_2(\mu)$  such that

$$\boldsymbol{\sigma}_{2,i}(\mu) \geq |\delta\mathbb{R}'_{\text{eig},i}(\mu)|. \quad (122)$$

We note that Proposition 1 holds for “any” candidate eigenpair and associated eigenproblem residual so long as the candidate eigenvector is  $\mathbb{B}'$ -normalized and the eigenvalue proximity assumption (80) holds. We may thus (under the proximity assumption) write

$$\lambda_{\min} \geq \tilde{\lambda}_{\text{A},\min} - \sqrt{(\mathbb{R}'_{\text{eig}})^{\text{T}}(\mathbb{B}')^{-1}\mathbb{R}'_{\text{eig}}} \quad (123)$$

$$= \tilde{\lambda}_{\text{A},\min} - \sqrt{(\tilde{\mathbb{R}}'_{\text{eig}})^{\text{T}}(\mathbb{B}')^{-1}\tilde{\mathbb{R}}'_{\text{eig}} + 2(\delta\mathbb{R}'_{\text{eig}})^{\text{T}}(\mathbb{B}')^{-1}\tilde{\mathbb{R}}'_{\text{eig}} + (\delta\mathbb{R}'_{\text{eig}})^{\text{T}}(\mathbb{B}')^{-1}\delta\mathbb{R}'_{\text{eig}}}, \quad (124)$$

(for simplicity we have omitted all  $\mu$  dependence). We now suppose that the constant  $C$  introduced in (118) is chosen large enough that

$$\delta\mathbb{R}'_{\text{eig}}(\mu)^{\text{T}}(\mathbb{B}')^{-1}\delta\mathbb{R}'_{\text{eig}}(\mu) \leq C\|\delta\mathbb{R}'_{\text{eig}}(\mu)\|_2^2. \quad (125)$$

From (124) and (122) we then obtain

$$\lambda_{\min, \text{LB}}(\mu) = \tilde{\lambda}_{\text{A},\min}(\mu) - \sqrt{(\tilde{\mathbb{R}}'_{\text{eig}})^{\text{T}}(\mathbb{B}')^{-1}\tilde{\mathbb{R}}'_{\text{eig}} + 2\boldsymbol{\sigma}_2(\mu)^{\text{T}}|(\mathbb{B}')^{-1}\tilde{\mathbb{R}}'_{\text{eig}}| + C\|\boldsymbol{\sigma}_2(\mu)\|_2^2} \quad (126)$$

which serves as our modified eigenvalue lower bound  $\lambda_{\min, \text{LB}}(\mu) \leq \lambda_{\min}(\mu)$ .



Now, from (119) and (126), we obtain the Schur energy bound

$$\|\mathbb{E}(\mu)\|_{\mathbb{A}(\mu)} \leq \Delta_{\mathbb{A}(\mu)}^{\mathbb{U}}(\mu; C) \equiv \sqrt{\frac{\tilde{\mathbb{R}}'(\mu)^{\mathbb{T}}(\mathbb{B}')^{-1}\tilde{\mathbb{R}}'(\mu) + 2\sigma_1(\mu)^{\mathbb{T}}(\mathbb{B}')^{-1}\tilde{\mathbb{R}}'(\mu) + C\|\sigma_1(\mu)\|_2^2}{\lambda_{\min, \text{LB}}(\mu)}}. \quad (127)$$

It thus remains to bound the energy  $\|e^h(\mu)\|_{\mu} = \|u^h(\mu) - \tilde{u}_A(\mu)\|_{\mu}$  in terms of  $\|\mathbb{E}(\mu)\|_{\mathbb{A}(\mu)}$ . To this end, we note that we may separate the  $\mathcal{S}$  and non- $\mathcal{S}$  parts of  $e^h(\mu)$  as

$$e^h(\mu) = \sum_{i=1}^I (b_i^{f;h}(\mu) - \tilde{b}_i^f(\mu)) + \sum_{p=1}^{n^{\Gamma}} \sum_{k=1}^{\mathcal{N}_p^{\Gamma}} (\mathbb{U}_{p,k}(\mu)\Phi_{p,k}(\mu) - \tilde{\mathbb{U}}_{A,p,k}(\mu)\tilde{\Phi}_{p,k}(\mu)) \quad (128)$$

$$= \sum_{i=1}^I (b_i^{f;h}(\mu) - \tilde{b}_i^f(\mu)) + \sum_{p=1}^{n^{\Gamma}} \sum_{k=1}^{\mathcal{N}_p^{\Gamma}} \left( \mathbb{E}_{p,k}(\mu)\Phi_{p,k}(\mu) + \tilde{\mathbb{U}}_{A,p,k}(\mu)(\Phi_{p,k}(\mu) - \tilde{\Phi}_{p,k}(\mu)) \right) \quad (129)$$

$$= \Delta b^f(\mu) + \Delta\Phi_A(\mu) + \underbrace{\sum_{p=1}^{n^{\Gamma}} \sum_{k=1}^{\mathcal{N}_p^{\Gamma}} \mathbb{E}_{p,k}(\mu)\Phi_{p,k}(\mu)}_{\in \mathcal{S}}, \quad (130)$$

where  $\Delta b^f(\mu)$  and  $\Delta\Phi_A(\mu)$  are given as

$$\Delta b^f(\mu) \equiv \sum_{i=1}^I (b_i^{f;h}(\mu) - \tilde{b}_i^f(\mu)), \quad \Delta\Phi_A(\mu) \equiv \sum_{p=1}^{n^{\Gamma}} \sum_{k=1}^{\mathcal{N}_{A,p}^{\Gamma}} \tilde{\mathbb{U}}_{A,p,k}(\mu)(\Phi_{p,k}(\mu) - \tilde{\Phi}_{p,k}(\mu)). \quad (131)$$

Thanks to the relation (41) we thus obtain

$$a(e^h(\mu), e^h(\mu); \mu) = \|\mathbb{E}(\mu)\|_{\mathbb{A}(\mu)}^2 + \|\Delta b^f(\mu) + \Delta\Phi_A(\mu)\|^2 + 2 \sum_{p=1}^{n^{\Gamma}} \sum_{k=1}^{\mathcal{N}_p^{\Gamma}} \mathbb{E}_{p,k}(\mu) a(\Phi_{p,k}(\mu), \Delta b^f(\mu) + \Delta\Phi_A(\mu); \mu); \quad (132)$$

and furthermore, thanks to (10) and (11), and the fact that  $(\Delta b^f(\mu) + \Delta\Phi_A(\mu))|_{\Omega_i} \in B_{\mathcal{M}(i);0}^h$ , we obtain

$$a(\Phi_{p,k}(\mu), \Delta b^f(\mu) + \Delta\Phi_A(\mu); \mu) = 0, \quad 1 \leq k \leq \mathcal{N}_p^{\Gamma}, 1 \leq p \leq n^{\Gamma}. \quad (133)$$

As a result

$$a(e^h(\mu), e^h(\mu); \mu) \leq \|\mathbb{E}(\mu)\|_{\mathbb{A}(\mu)}^2 + \sigma_3(\mu)^2, \quad (134)$$

where

$$\sigma_3(\mu) \geq \|\Delta b^f(\mu) + \Delta\Phi_A(\mu)\|_{\mu} \quad (135)$$

is readily obtained from standard RB bubble function error bounds.

With  $\Delta_{\mathbb{A}(\mu)}^{\mathbb{U}}(\mu; C)$  in (127) we may now *redefine* our error bound in Proposition 2 as

$$\Delta^u(\mu) \equiv \sqrt{(\Delta_{\mathbb{A}(\mu)}^{\mathbb{U}}(\mu; C))^2 + \sigma_3(\mu)^2} \quad (136)$$

for which

$$\|u^h(\mu) - \tilde{u}_A(\mu)\|_{\mu} \leq \Delta^u(\mu). \quad (137)$$

It remains to bound the constant  $C$ .

We note that as  $\sigma_{1,i}, \sigma_{2,i} \rightarrow 0$ , we may neglect second-order terms in (127) to obtain an asymptotic Schur energy bound  $\Delta_{\mathbb{A}(\mu),\text{asy}}^{\mathbb{U}}(\mu) \sim \Delta_{\mathbb{A}(\mu)}^{\mathbb{U}}(\mu; C)$  as

$$\Delta_{\mathbb{A}(\mu),\text{asy}}^{\mathbb{U}}(\mu) \equiv \sqrt{\frac{\tilde{\mathbb{R}}'(\mu)^{\text{T}}(\mathbb{B}')^{-1}\tilde{\mathbb{R}}'(\mu) + 2\sigma_1(\mu)^{\text{T}}(\mathbb{B}')^{-1}\tilde{\mathbb{R}}'(\mu)}{\tilde{\lambda}_{\mathbb{A},\text{min}}(\mu) - \sqrt{(\tilde{\mathbb{R}}'_{\text{eig}})^{\text{T}}(\mathbb{B}')^{-1}\tilde{\mathbb{R}}'_{\text{eig}} + 2\sigma_2(\mu)^{\text{T}}(\mathbb{B}')^{-1}\tilde{\mathbb{R}}'_{\text{eig}}}}}; \quad (138)$$

furthermore, as  $\sigma_3 \rightarrow 0$ , we may neglect the  $\sigma_3(\mu)^2$ -term in (134) to obtain an asymptotic field energy bound  $\Delta_{\text{asy}}^u(\mu) \sim \Delta^u(\mu)$  as

$$\Delta_{\text{asy}}^u(\mu) \equiv \Delta_{\mathbb{A}(\mu),\text{asy}}^{\mathbb{U}}(\mu). \quad (139)$$

We now note that  $C$  no longer appears. Alternatively, we may compute the smallest eigenvalue  $\lambda_{\text{min}}^{\mathbb{B}'}$  of  $\mathbb{B}'$  — efficiently realized through an inverse power iteration or inverse Lanczos procedure, in which case we only require a few additional non-conforming  $\mathbb{B}'$ -solves — and choose  $C = 1/\lambda_{\text{min}}^{\mathbb{B}'}$ ;<sup>12</sup> or we may compute a lower bound  $\lambda_{\text{min, LB}}^{\mathbb{B}'} \leq \lambda_{\text{min}}^{\mathbb{B}'}$  — per the procedures in Section 4.4 through consideration of the generalized eigenproblem with  $\mathbb{B}'$  as the left-hand-side matrix and the identity as the right-hand-side matrix — and choose  $C = 1/\lambda_{\text{min, LB}}^{\mathbb{B}'}$ . In actual (computational) practice we thus have two options: we may either realize the rigorous (under the eigenvalue proximity assumption (80)) bound  $\Delta^u(\mu)$  by computing  $\lambda_{\text{min}}^{\mathbb{B}'}$  (or  $\lambda_{\text{min, LB}}^{\mathbb{B}'}$ ) or we may assume that our RB error bounds are sufficiently small that the asymptotically rigorous bound  $\Delta_{\text{asy}}^u(\mu)$  is acceptable. Note that in either case we must ensure that  $\lambda_{\text{min, LB}}(\mu)$  is positive or of course no bound may be calculated: the RB errors must be sufficiently small to preserve stability.

Finally, we note that armed with this new bound (in the case of  $\Delta^u(\mu)$ ) or estimator (in the case of  $\Delta_{\text{asy}}^u(\mu)$ ), Corollary 1 for compliance outputs extends directly to the case of non-zero RB errors thanks to Galerkin orthogonality of  $e^h(\mu)$  with respect to  $\tilde{\mathcal{S}}_{\mathbb{A}} \subset X^h(\Omega)$ . Analogous to (50) we thus obtain

$$|s^h(\mu) - \tilde{s}_{\mathbb{A}}(\mu)| = a(e^h(\mu), e^h(\mu); \mu) \leq (\Delta^u(\mu))^2; \quad (140)$$

and

$$|s^h(\mu) - \tilde{s}_{\mathbb{A}}(\mu)| \lesssim (\Delta_{\text{asy}}^u(\mu))^2 + \mathcal{O}(\sigma_{1,i}^2(\mu) + \sigma_{2,i}^2 + \sigma_3^2), \quad (141)$$

respectively. In the results of Section 6 we apply (140) for  $C = 1/\lambda_{\text{min, LB}}^{\mathbb{B}'}$ .

We do not in the current paper consider error contribution from RB bubble approximation to the non-compliance output bounds given in (96).

## References

- [1] H. Antil, M. Heinkenschloss, and R. H.W. Hoppe. Domain decomposition and balanced truncation model reduction for shape optimization of the stokes system. *Optimization Methods and Software*, 26(4-5):643–669, 2011.
- [2] P. F. Batcho and G. Em. Karniadakis. Generalized Stokes eigenfunctions: a new trial basis for the solution of incompressible Navier-Stokes equations. *J. Comput. Phys.*, 115(1):121–146, 1994.
- [3] A. Bermúdez and F. Pena. Galerkin lumped parameter methods for transient problems. *Internat. J. Numer. Methods Engrg.*, 87(10):943–961, 2011.
- [4] C. Bernardi and Y. Maday. Spectral methods. In *Handbook of numerical analysis*, volume V, pages 209–485. North-Holland, 1997.

---

<sup>12</sup>Note that this direct method is applicable to  $\lambda_{\text{min}}^{\mathbb{B}'}$  and not to  $\lambda_{\text{min}}(\mu)$  because for the latter we do not form the  $\mathbb{A}_{\text{II}}^i(\mu)$  component-local matrix blocks.

- [5] C. Bernardi, Y. Maday, and A. T. Patera. A new nonconforming approach to domain decomposition: the mortar element method. In *Nonlinear partial differential equations and their applications. Collège de France Seminar, Vol. XI (Paris, 1989–1991)*, volume 299 of *Pitman Res. Notes Math. Ser.*, pages 13–51. Longman Sci. Tech., Harlow, 1994.
- [6] F. Bourquin. Component mode synthesis and eigenvalues of second order operators: Discretization and algorithm. *Mathematical Modelling and Numerical Analysis*, 26(3):385–423, 1992.
- [7] S. C. Brenner. The condition number of the Schur complement in domain decomposition. *Numer. Math.*, 83(2):187–203, 1999.
- [8] P. G. Ciarlet. Basic error estimates for elliptic problems. In *Handbook of numerical analysis, Vol. II*, *Handb. Numer. Anal.*, II, pages 17–351. North-Holland, Amsterdam, 1991.
- [9] R. Craig and M. Bampton. Coupling of substructures for dynamic analyses. *AIAA J*, 6(7):1313–1319, 1968.
- [10] J. L. Eftang, D. B. P. Huynh, D. J. Knezevic, E. M. Rønquist, and A. T. Patera. Adaptive port reduction in static condensation. In *7th Vienna International Conference on Mathematical Modelling*, 2013.
- [11] J. L. Eftang and E. M. Rønquist. Evaluation of flux integral outputs for the reduced basis method. *Math. Models Methods Appl. Sci.*, 20(3):351–374, 2010.
- [12] U. L. Hetmaniuk and R. B. Lehoucq. A special finite element method based on component mode synthesis. *M2AN Math. Model. Numer. Anal.*, 44(3):401–420, 2010.
- [13] W. C. Hurty. On the dynamic analysis of structural systems using component modes. In *First AIAA Annual meeting, Washington, June 29 — July 2 1964*. AIAA paper, no. 64-487.
- [14] D. B. P. Huynh. A static condensation reduced basis element approximation: Application to three-dimensional acoustic muffler analysis. In *Proceedings of the International Conference on Advances in Computational Mechanics (to appear)*, 2012.
- [15] D. B. P. Huynh, D. J. Knezevic, and A. T. Patera. A static condensation reduced basis element method: Approximation and a posteriori error estimation. *Mathematical Modelling and Numerical Analysis*, 47(1):213–251, 2013.
- [16] D. B. P. Huynh, D. J. Knezevic, and A. T. Patera. A static condensation reduced basis element method: Complex problems. *Computer Methods in Applied Mechanics and Engineering (accepted)*, 2013.
- [17] E. Isaacson and H. B. Keller. *Computation of Eigenvalues and Eigenvectors, Analysis of Numerical Methods*. Dover, New York, 1994.
- [18] H. Jakobsson, F. Bengzon, and M. G. Larson. Adaptive component mode synthesis in linear elasticity. *Internat. J. Numer. Methods Engrg.*, 86(7):829–844, 2011.
- [19] K. Kunisch and S. Volkwein. Galerkin proper orthogonal decomposition methods for a general equation in fluid dynamics. *SIAM J. Numer. Anal.*, 40(2):492–515 (electronic), 2002.
- [20] Y. Maday and E. M. Rønquist. A reduced basis element method. *Journal of Scientific Computing*, 17:447–459, 2002.
- [21] Y. Maday and E. M. Rønquist. The reduced-basis element method: application to a thermal fin problem. *SIAM Journal on Scientific Computing*, 26(1):240–258, 2004.
- [22] A. T. Patera. A spectral element method for fluid dynamics: Laminar flow in a channel expansion. *Journal of Computational Physics*, 54(3):468 – 488, 1984.

- [23] N. A. Pierce and M. B. Giles. Adjoint recovery of superconvergent functionals from PDE approximations. *SIAM Review*, 42(2):247–264, 2000.
- [24] A. Quarteroni and A. Valli. *Numerical approximation of partial differential equations*, volume 23 of *Springer Series in Computational Mathematics*. Springer-Verlag, Berlin, 1994.
- [25] G. Rozza, D. B. P. Huynh, and A. T. Patera. Reduced basis approximation and a posteriori error estimation for affinely parametrized elliptic coercive partial differential equations: application to transport and continuum mechanics. *Archives of Computational Methods in Engineering*, 15(3):229–275, 2008.
- [26] G. Strang. *Linear algebra and its applications*. Academic Press, New York, second edition, 1980.
- [27] A. Toselli and O. Widlund. *Domain decomposition methods—algorithms and theory*, volume 34 of *Springer Series in Computational Mathematics*. Springer-Verlag, Berlin, 2005.
- [28] S. Vallagé and A. T. Patera. The static condensation reduced basis element method for a mixed-mean conjugate heat exchanger model. *SIAM Journal on Scientific Computing (submitted)*, 2012.
- [29] K. Veroy, D. V. Rovas, and A. T. Patera. A posteriori error estimation for reduced-basis approximation of parametrized elliptic coercive partial differential equations: “convex inverse” bound conditioners. *ESAIM: Control, Optimisation and Calculus of Variations*, 8:1007–1028, 2002.